ARTHRITIS & RHEUMATISM
Vol. 52, No. 2, February 2005, pp 637–641
DOI 10.1002/art.20794

Use of Local Electroporation Enhances Methotrexate Effects With Minimum Dose in Adjuvant-Induced Arthritis

Masahiro Tada, Kentaro Inui, Tatsuya Koike, and Kunio Takaoka

Objective. **To investigate the effects of electrical pulses on the ability of methotrexate (MTX) to attenuate inflammation and subsequent joint destruction in rats with adjuvant-induced arthritis (AIA).**

Methods. **Rats in the experimental group received an intraperitoneal injection of MTX (0.125 mg/kg body weight), followed 30 minutes later by application of direct electrical pulses (50V, 8 Hz) to their left hind paws with an electroporation apparatus (M+/E+ group; n = 8). The procedure was repeated twice weekly for 3 weeks. Three control groups received the following treatments, respectively: MTX without electrical treatment (M+/E− group; n = 9), electrical treatment but no MTX (M−/E+ group; n = 10), or no electrical treatment and no MTX (M−/E− group; n = 9). Progression of AIA was monitored by joint swelling and radiologic and histologic changes in the ankle joint.**

Results. **Three weeks after injection of the adjuvant, and at the height of the arthritic reaction, the swelling and radiologic and histologic changes in the left hind paws in the M+/E+ rats were significantly reduced, as compared with changes observed in the control groups.**

Conclusion. **These results demonstrate that application of electrical pulses in combination with use of systemic low-dose MTX can ameliorate local arthritic reactions. This response probably occurs because electrical stimulation promotes transient passage of MTX through pores in the cell membranes, with a resultant local increase in the concentration of the drug within the cells. These results point to a potential use of electrochemotherapy to increase the efficacy of MTX or other drugs in an arthritic joint that is refractory to treatment, without increasing the dose of the drug.**

Although new biologic agents (1) can ameliorate inflammatory reactions and consequently protect the joints of patients with rheumatoid disease from progressive damage (2), methotrexate (MTX) remains one of the most effective and widely used disease-modifying antirheumatic drugs (DMARDs) (3). However, chronic inflammation often persists in isolated joints even after effective systemic MTX treatment, presumably as a result of an inadequate concentration of MTX in the joint that is refractory to treatment. In patients with persistent inflammation, synovectomy is often indicated for symptomatic relief, although data on the long-term clinical effectiveness of this approach are limited (4). Another option is an additional dose of MTX, but this increases the risk of adverse events. Because MTX has weak cell permeability, and the pharmacologic effects of this drug depend upon its intracellular concentration, any method for increasing intracellular MTX levels in the joint may be effective in attenuating the inflammatory response.

Electroporation has been used to facilitate the transport of nonpermeable molecules into cells. Transient cell membrane pores, generated electrically, allow nonpermeable molecules, including genes and drugs, to enter into the cells (5). Electroporation systems are now available for clinical use to deliver anticancer drugs into malignant solid tumor cells (6–8) as electrochemotherapy. Encouraging clinical results have been reported for the treatment of malignancies, in terms of efficacy, safety, and cost (9). This suggests that electroporation may be useful for the local treatment of rheumatoid arthritis (RA) that is refractory to conventional therapy.

We used electroporation to enhance the effect of

Supported by the Ministry of Education, Culture, Sports, Science and Technology of Japan (grant-in-aid 15591594).

Masahiro Tada, MD, Kentaro Inui, MD, PhD, Tatsuya Koike, MD, PhD, Kunio Takaoka, MD, PhD: Osaka City University, Graduate School of Medicine, Osaka, Japan.

Address correspondence and reprint requests to Masahiro Tada, MD, Department of Orthopaedic Surgery, Osaka City University, Graduate School of Medicine, 1-4-3 Asahimachi, Abeno-ku, Osaka 545-8585, Japan. E-mail: m-tada@med.osaka-cu.ac.jp.

Submitted for publication May 11, 2004; accepted in revised form October 21, 2004.

low-dose MTX treatment on the progression to severe arthritis and associated joint destruction in a rat model of adjuvant-induced arthritis (AIA) (10–12).

MATERIALS AND METHODS

Animals. Inbred 7-week-old male Lewis rats were purchased from Charles River Japan (Kanagawa, Japan) and housed with free access to standard laboratory chow and water, under 12-hour dark/light cycles in conditioned air.

Induction of arthritis. The adjuvant mixture was prepared by mixing dried heat-killed *Mycobacterium butyricum* (Difco, Detroit, MI) in paraffin oil (Wako, Tokyo, Japan) at a concentration of 5 mg/ml. To induce systemic arthritis, 0.2 ml of the preparation was injected into the tail bases of 8-week-old rats that had received anesthesia via ethyl ether inhalation.

Pulsed electrical stimulation for electroporation. For electrical stimulation to generate transient pores in cell membranes at the target tissue site, we used an electroporation apparatus (CUY-21; Gene System, Osaka, Japan). Direct-current electrical pulses (8 Hz, 75 msec pulse duration, 50 volts/cm electrode distance) of 1-second duration were delivered 6 times during a single procedure. Each of the six 1-second pulses was applied by 2 parallel stainless steel electrodes that were moved between each pulse through 60° in a plane perpendicular to the long axis of the left hind paws, 30 minutes after an intraperitoneal injection of MTX or saline. We used electrode paste (Gelaid; Nihon Koden, Tokyo, Japan) to prevent skin burns.

Experimental protocol. The animals were assigned to an experimental group or to 1 of 3 control groups, as follows: MTX injection with electroporation (M+/E+ [experimental] group; n = 8), MTX without electroporation (M+/E− group; n = 9), electroporation with saline (M−/E+ group; n = 10), or no treatment (M−/E− group; n = 9).

MTX was provided by Wyeth-Pharmaceutical (Tokyo, Japan). The dose of MTX was set to 0.125 mg/kg body weight, based on preliminary experimental data indicating that no significant systemic antiarthritic changes were recognized at this dose. The drug was administered intraperitoneally twice weekly for 3 weeks, and the animals were killed by asphyxia in carbon dioxide (for radiologic and histologic examination).

These experimental protocols were in accordance with institutional regulations for animal care and were approved by the Institutional Committee for Animal Care of Osaka City University.

Gross inspection and radiologic evaluation. Twice weekly, the animals were weighed using an electronic balance, and hind paw thickness was measured with digital calipers. Three weeks after the adjuvant was injected, the animals were killed using CO_2 asphyxiation, and both hind limbs were harvested and fixed by perfusing cold 4% paraformaldehyde through the left ventricle, followed by immersion in cold 4% paraformaldehyde solution. Soft x-ray images of the hind paws were obtained with a soft x-ray apparatus (DCS-600EX; Aloka, Tokyo, Japan) using settings of 45 kV, 4 mA, and 30 seconds of exposure time. Destructive changes in hind paw bones seen on radiographs were evaluated by criteria previously described by Clark et al (13), with some modifications. Briefly, radiographic

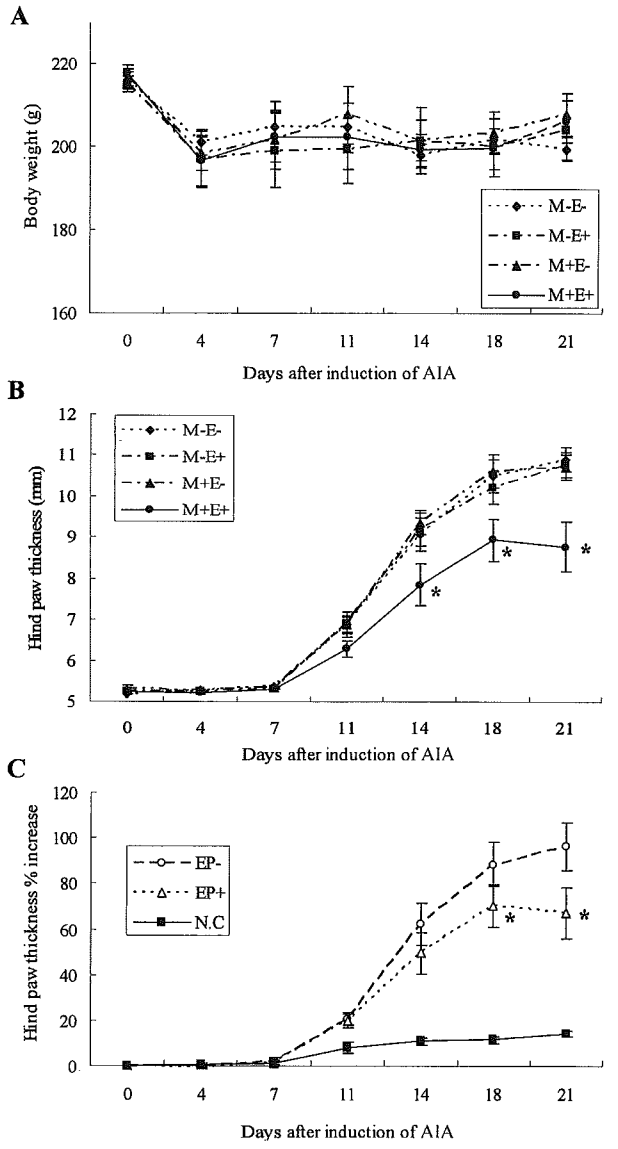

Figure 1. Effects of electrochemotherapy with methotrexate (MTX) on body weight and paw swelling in rats with adjuvant-induced arthritis (AIA). **A,** Weight loss was observed in all groups on day 4. There was no significant weight difference between the 4 groups throughout the entire study period. **B,** Left hind paw thickness, as measured by digital calipers, was maximal on day 21 in the M−/E− (no treatment; n = 9), M−/E+ (electroporation with saline; n = 10), and M+/E− (MTX without electroporation; n = 9) groups. The thickness of the left hind paw treated with electrical pulses after administration of MTX, 0.125 mg/kg/week (M+/E+; n = 8) was significantly decreased when compared with the other groups. * = $P < 0.05$ versus the M−/E−, M−/E+, and M+/E− groups. **C,** Effects of electrical pulses on paw swelling in the M+/E+ group. Electrical pulses were applied to the left hind paw only (electrically treated [EP+]) (n = 8), not the right paw (not electrically treated [EP−]) (n = 8). Application of electrical pulses after administration of low-dose MTX significantly inhibited hind paw swelling on days 18 and 21, as assessed by paw thickness and when compared with EP− paws. NC = negative control (non–adjuvant-injected model) (n = 5). * = $P < 0.05$ versus EP−. Bars show the mean ± SEM.

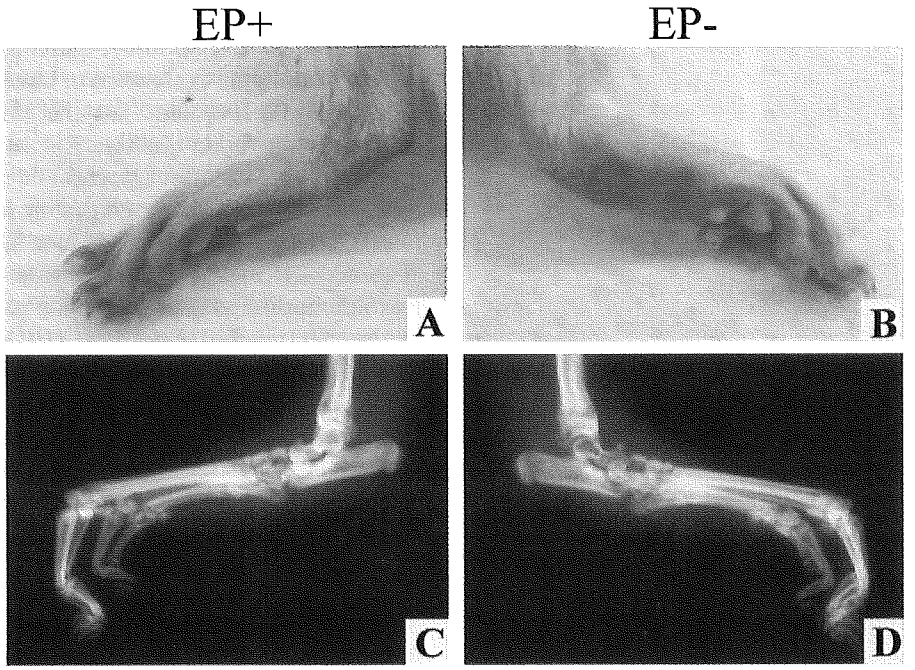

Figure 2. Gross appearance and radiographs of the hind paws of the same rat in the M+/E+ group on day 21. Following administration of MTX (0.125 mg/kg/week), electrical pulses were applied to the left hind paw only (EP+) (**A** and **C**). Note the obvious difference in the degree of swelling and joint damage between the left paw (EP+) and right paw (EP−) in gross appearance (**A** and **B**), as well as on soft x-ray (**C** and **D**). See Figure 1 for definitions.

changes in terms of radiodensity, subchondral bone erosion, periosteal reaction, and cartilage space were evaluated under blinded conditions by 2 rheumatologists (KI and TK) and graded on a 0–3 scale (where 0 = normal and 3 = severely damaged).

Histologic sections. Both hind paws were harvested from the animals for histopathologic examination. After the removal of skin, bones in the hind paws were decalcified in a neutral buffered 14% solution of EDTA/10% formalin, dehydrated in a graded ethanol series, embedded in paraffin, sectioned sagittally into 4-μm sections, and stained with hematoxylin and eosin or toluidine blue. Pathologic changes were evaluated by 2 observers according to a previously reported rating system (14), as follows: grade 0 = normal synovium, cartilage, and bone; grade 1 = hypertrophic synovium with cellular infiltration without pathologic change in bone and cartilage; grade 2 = pannus formation and cartilage erosion in addition to the hypertrophic synovium; grade 3 = additional severe erosion of cartilage and subchondral bone; grade 4 = loss of joint integrity and ankylosis.

In order to identify and count osteoclastic cells, sections were stained for tartrate-resistant acid phosphate (TRAP) using a staining kit (Sigma-Aldrich, St. Louis, MO). TRAP-positive multinucleated cells were counted in 11 selected fields (8 fields in the distal tibia and 3 fields in the talus), all at 100× magnification.

Statistical analysis. Body weight and hind paw thickness were evaluated by repeated analysis of variance and Fisher's protected least significant difference test. Pairwise comparisons were made using Wilcoxon's signed rank tests among groups. All statistical analyses were carried out using StatView software version 5.0 (SAS Institute, Cary, NC). P values less than or equal to 0.05 were considered significant.

RESULTS

Effects of electrochemotherapy on progression of AIA. No significant difference in body weight was noted between the 4 groups during the course of this experiment (Figure 1A), indicating that low-dose MTX, with or without electroporation, had little effect on the systemic physical condition of the rats with AIA.

The thickness of the hind paws in all rats was

Table 1. Radiologic and histologic scores and osteoclast numbers in rat AIA, 21 days after injection of adjuvant*

Group	Radiologic score (n = 8)	Histologic score (n = 8)	Osteoclast number (n = 5)
Right hind paw, EP-negative	3.8 ± 4.5	2.5 ± 1.2	77.6 ± 10.2
Left hind paw, EP-positive†	1.8 ± 2.2	1.3 ± 0.5	22.0 ± 2.4

* Values are the mean ± SD. AIA = adjuvant-induced arthritis; EP = electroporation.
† For all comparisons, $P < 0.05$ versus EP-negative.

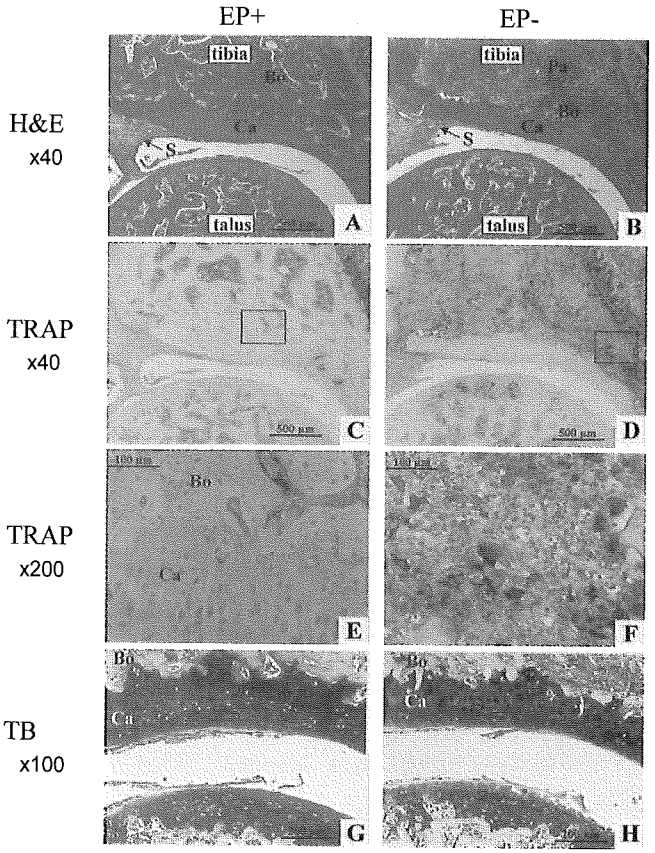

Figure 3. Histologic analysis of the ankle joints of the same rat in the M+/E+ group on day 21. **A** and **B,** Staining with hematoxylin and eosin (H&E). **C, D, E,** and **F,** Staining with tartrate-resistant acid phosphate (TRAP). **G** and **H,** Staining with toluidine blue (TB). The electroporation procedure was applied to the left ankle joint only (EP+) (**A, C, E,** and **G**). No inflammatory synovial tissue erosion into subchondral bone was observed with application of electroporation (**A**) compared with MTX only (**B**). Inflamed synovium infiltrated with lymphocytes was found to contain abundant osteoclastic multinucleated cells on TRAP staining (**D** and **F**). However, there was no difference in metachromasia of articular cartilage in the left and right hind paws. **E,** Higher-magnification view of the boxed area in **C. F,** Higher-magnification view of the boxed area in **D.** Bo = subchondral bone; Ca = cartilage; Pa = pannus; S = synovial tissue (see Figure 1 for other definitions).

significantly and consistently increased from day 11 until the end of the experiment. However, in the M+/E+ group, swelling of the left hind paw was significantly suppressed on days 14, 18, and 21 (Figure 1B) when compared with the 3 control groups (M+/E−, M−/E+, and M−/E−). The gross appearance of the hind paws is shown in Figures 2A and B. Thus, application of electrical pulses appeared to prevent the hind paw joints from progressing to advanced AIA. The degree of swelling differed significantly between the left (electrically treated [EP+]) and right (EP−) paws of the same rat in the M+/E+ group (Figure 1C).

Radiologic evaluation of bones and joints. Radiologic analysis revealed that the hind paw joints were severely damaged in the M−/E−, M−/E+, and M+/E− groups at 21 days after injection of the adjuvant. Therefore, at a dose of 0.125 mg/kg body weight, MTX did not prevent the joint damage (Figure 2D) or local swelling (Figure 2B) caused by progression of arthritis. In contrast, the radiologic damage score was significantly lower in the electrically treated left (EP+) hind paws in the M+/E+ group (Figures 2A and C and Table 1).

Histologic analyses. In the M+/E+ group, the histologic scores were significantly lower in the left hind paws (EP+) than in the right hind paws (EP−) (Figures 3A and B and Table 1). Inflamed synovial tissues with abundant lymphocytes were observed to erode into subchondral bone (Figure 3B). In sections of these joints, the population of TRAP-positive multinucleated osteoclastic cells was significantly lower in the bones of the left hind paw (EP+) than in those of the right hind paw (EP−) (Figures 3C, D, E, and F and Table 1). Toluidine blue staining revealed no degenerative changes of cartilage tissue, including irregularity of articular surface, disorganization of tidemark, and alternation of metachromasia, in either hind paw (Figures 3G and H).

DISCUSSION

These results indicate positive effects of pulsed electrical stimulation for attenuating arthritis by enhancing the antiarthritic effect of MTX. We believe that this is attributable to micropores created by the electrical pulses in the cytoplasmic membranes of cells in the synovium or other inflamed cells. The subsequent passive influx of MTX into the cells would attenuate the inflammatory responses that led to the AIA, although this study did not provide direct evidence of MTX influx. In this preliminary study, we could not identify the cells targeted by electrochemotherapy, and MTX-negative synovial cells, inflammatory cells, or both, may be targets for the drug.

The effects of electrical fields on living cells have been investigated since the 1960s, and high-voltage electrical pulses have been reported to generate transient and reversible pores in cell membranes. This phenomenon has been termed electroporation and is currently used to transfer genes or drugs into cells (6). Electrochemotherapy involves electroporation with drugs, and this methodology is used for the treatment of malignant tumors (5–9). The use of electrochemotherapy to introduce anticancer drugs into malignant tumors has been reported, e.g., bleomycin

for melanoma, basal cell carcinoma, Kaposi's sarcoma, squamous cell carcinoma (6), or chondrosarcoma (15). However, electrochemotherapy with MTX for the treatment of RA has not been reported, although the less-permeable character of MTX and its use as a DMARD in RA would make it an ideal candidate for this approach. Because the effect of pulsed electrical stimulation is expected only at the local site, this method might be applicable for an isolated joint with arthritis that is refractory to systemic chemotherapy or in the early stages of RA involving a limited number of joints without significant joint-destructive changes.

Clinical application of this therapy should not affect normal tissues. Using TUNEL staining, we did not observed any difference in the number of apoptotic cells between the M+/E+ and M+/E− groups (data not shown). We also confirmed in the pilot study that electrical pulses, used under the same conditions as those used in this experiment, did not influence the normal tissues of inbred 9-week-old male Lewis rats. In this pilot study, no inflammatory reactions were observed on histologic examination of the area treated with the electrical pulses, suggesting that electroporation under these conditions did not cause any damage to normal tissue, including cartilage, bone, muscle, and blood vessels (results not shown). However, the clinical application of electrochemotherapy requires further study, including the dose of MTX and the parameters of the electrical pulses.

This experimental study is limited in 2 key areas. First, electrochemotherapy was not applied to joints with established arthritis, and the effect of electrochemotherapy was estimated based on the progression of arthritis. This differs from the clinical situation, in which, as indicated previously (10,11), the inflammatory phase in this AIA model is self-limiting. Therefore, the efficacy of electrochemotherapy for the treatment of established chronic arthritis is difficult to determine in this model. Second, optimization of the application of pulsed electrical current may not be sufficient to obtain maximum delivery of MTX into cells and to achieve maximal antiinflammatory effect in RA. The conditions that enable the efficacy of electrical stimulation in electrochemotherapy may be quite different from the conditions used in the clinical treatment of malignancies that were reference sources for the present study. The potential value of electrochemotherapy for the treatment of RA has been illustrated by these studies, and further work is required to optimize electrochemotherapy to control disease in joints with RA refractory to treatment.

REFERENCES

1. Maini R, St Clair EW, Breedveld F, Furst D, Kalden J, Weisman M, et al, and the ATTRACT Study Group. Infliximab (chimeric anti-tumour necrosis factor α monoclonal antibody) versus placebo in rheumatoid arthritis patients receiving concomitant methotrexate: a randomised phase III trial. Lancet 1999;354:1932–9.
2. Lipsky PE, van der Heijde DM, St Clair EW, Furst DE, Breedveld FC, Kalden JR, et al, and the Anti-Tumor Necrosis Factor Trial in Rheumatoid Arthritis with Concomitant Therapy Study Group. Infliximab and methotrexate in the treatment of rheumatoid arthritis. N Engl J Med 2000;343:1594–602.
3. Furst DE, Kremer JM. Methotrexate in rheumatoid arthritis. Arthritis Rheum 1988;31:305–14.
4. Multicenter evaluation of synovectomy in the treatment of rheumatoid arthritis: report of results at the end of three years. Arthritis Rheum 1977;20:765–71.
5. Heller R, Gilbert R, Jaroszeski MJ. Clinical applications of electrochemotherapy. Adv Drug Deliv Rev 1999;35:119–29.
6. Mir LM, Orlowski S. Mechanisms of electrochemotherapy. Adv Drug Deliv Rev 1999;35:107–18.
7. Hyacinthe M, Jaroszeski MJ, Dang VV, Coppola D, Karl RC, Gilbert RA, et al. Electrically enhanced drug delivery for the treatment of soft tissue sarcoma. Cancer 1999;85:409–17.
8. Horiuchi A, Nikaido T, Mitsushita J, Toki T, Konishi I, Fujii S. Enhancement of antitumor effect of bleomycin by low-voltage in vivo electroporation: a study of human uterine leiomyosarcomas in nude mice. Int J Cancer 2000;88:640–4.
9. Gothelf A, Mir LM, Gehl J. Electrochemotherapy: results of cancer treatment using enhanced delivery of bleomycin by electroporation. Cancer Treat Rev 2003;29:371–87.
10. Welles WL, Silkworth J, Oronsky AL, Kerwar SS, Galivan J. Studies on the effect of low dose methotrexate on rat adjuvant arthritis. J Rheumatol 1985;12:904–6.
11. Kawai S, Nagai K, Nishida S, Sakyo K, Murai E, Mizushima Y. Low-dose pulse methotrexate inhibits articular destruction of adjuvant arthritis in rats. J Pharm Pharmacol 1997;49:213–5.
12. Morgan SL, Baggott JE, Bernreuter WK, Gay RE, Arani R, Alarcon GS. MTX affects inflammation and tissue destruction differently in the rat AA model. J Rheumatol 2001;28:1476–81.
13. Clark RL, Cuttino JT Jr, Anderle SK, Cromartie WJ, Schwab JH. Radiologic analysis of arthritis in rats after systemic injection of streptococcal cell walls. Arthritis Rheum 1979;22:25–35.
14. Shiozawa S, Shimizu K, Tanaka K, Hino K. Studies on the contribution of c-fos/AP-1 to arthritic joint destruction. J Clin Invest 1997;99:1210–6.
15. Shimizu T, Nikaido T, Gomyo H, Yoshimura Y, Horiuchi A, Isobe K, et al. Electrochemotherapy for digital chondrosarcoma. J Orthop Sci 2003;8:248–51.

OsteoArthritis and Cartilage (2005) **13,** 405–417

doi:10.1016/j.joca.2004.12.014

Osteoarthritis and Cartilage | ICRS International Cartilage Repair Society | OA OSTEOARTHRITIS

A new biotechnology for articular cartilage repair: subchondral implantation of a composite of interconnected porous hydroxyapatite, synthetic polymer (PLA-PEG), and bone morphogenetic protein-2 (rhBMP-2)

Noriyuki Tamai M.D., Ph.D.†, Akira Myoui M.D., Ph.D.†, Makoto Hirao M.D.†, Takashi Kaito M.D.†, Takahiro Ochi M.D., Ph.D.‡, Junzo Tanaka Ph.D.§, Kunio Takaoka M.D., Ph.D.‖ and Hideki Yoshikawa M.D., Ph.D.†*

† *Department of Orthopaedic Surgery, Osaka University Graduate School of Medicine, 2-2 Yamadaoka, Suita, Osaka 565-0871, Japan*

‡ *National Hospital Organization Sagamihara National Hospital, 18-1 Sakuradai, Sagamihara, Kanagawa 228-8522, Japan*

§ *Biomaterials Center, National Institute for Materials Science, 1-1 Namiki, Tsukuba, Ibaraki 305-0044, Japan*

‖ *Department of Orthopaedic Surgery, Osaka City University Medical School, 1-4-3 Asahimachi, Abeno-ku, Osaka 545-8585, Japan*

Summary

Objective: Articular cartilage repair remains a major obstacle in tissue engineering. We recently developed a novel tool for articular cartilage repair, consisting of a triple composite of an interconnected porous hydroxyapatite (IP-CHA), recombinant human bone morphogenetic protein-2 (rhBMP-2), and a synthetic biodegradable polymer [poly-D,L-lactic acid/polyethylene glycol (PLA-PEG)] as a carrier for rhBMP-2. In the present study, we evaluated the capacity of the triple composite to induce the regeneration of articular cartilage.

Methods: Full-thickness cartilage defects were created in the trochlear groove of 52 New Zealand White rabbits. Sixteen defects were filled with the bone morphogenetic protein (BMP)/PLA–PEG/IP-CHA composite (group I), 12 with PLA–PEG/IP-CHA (group II), 12 with IP-CHA alone (group III), and 12 were left empty (group IV). The animals were killed 1, 3, and 6 weeks after surgery, and the gross appearance of the defect sites was assessed. The harvested tissues were examined radiographically and histologically.

Results: One week after implantation with the BMP/PLA–PEG/IP-CHA composite (group I), vigorous repair had occurred in the subchondral defect. It contained an agglomeration of mesenchymal cells which had migrated from the surrounding bone marrow either directly, or indirectly via the interconnecting pores of the IP-CHA scaffold. At 6 weeks, these defects were completely repaired. The regenerated cartilage manifested a hyaline-like appearance, with a mature matrix and a columnar organization of chondrocytes.

Conclusions: The triple composite of rhBMP-2, PLA-PEG, and IP-CHA promotes the repair of full-thickness articular cartilage defects within as short a period as 3 weeks in the rabbit model. Hence, this novel cell-free implant biotechnology could mark a new development in the field of articular cartilage repair.

Key words: Articular cartilage repair, Interconnected porous hydroxyapatite (IP-CHA), BMP, PLA-PEG.

Introduction

To date, the myth "once destroyed, cartilage cannot be repaired" has yet to be dispelled[1]. Mature articular cartilage cannot heal spontaneously owing to its low mitotic activity, which contrasts to the rapid rate of chondrocytic mitosis during normal cartilage growth.

Recently, several researchers have attempted to utilize culture-expanded autologous chondrocytes in combination with collagen sponges or fibrin glue to effect the repair of cartilage defects[2,3]. However, the results were either unsatisfactory or, if satisfactory, were achieved only after a lengthy wait for the regeneration of hyaline cartilage[2,4]. These poor results may reflect the characteristics of the transplantation technique, which involves the application of cartilage-derived cells to the defect[5].

Mesenchymal stem cells (MSCs) isolated from bone marrow have the ability to differentiate into chondrocytes, osteoblasts and other connective tissue cells of mesenchymal origin when cultured under appropriate *in vitro* conditions[6,7]. In an effort to exploit the pluripotentiality of MSCs, MSC-based repair strategies have been instigated in rabbits and goats, but with limited success[8,9]. Clinically,

*Address correspondence and reprint requests to: Hideki Yoshikawa. Tel: 81-6-6879-3552; Fax: 81-6-6879-3559; E-mail: yhideki@ort.med.osaka-u.ac.jp
Received 8 November 2004; revision accepted 20 December 2004.

surgical interventions, such as microfracturing, abrasion arthroplasty and osteochondral drilling, have been widely used and considered to be partially successful[10,11]. These techniques are based on the concept that intentional damage to the subchondral bone recruits MSCs to the defect, thereby promoting cartilage repair.

A potentially powerful alternative approach for cartilage regeneration is the local administration of bone morphogenetic proteins (BMPs), which are members of the transforming growth factor-β superfamily. BMPs have been shown to regulate and promote the growth and differentiation of chondrocytes, osteoblasts and MSCs[12,13]. Indeed, recombinant human bone morphogenetic protein-2 (rhBMP-2) can stimulate the *in vitro* synthesis of components of the chondrocytic matrix, such as proteoglycans and type-II collagen[14–16]. Furthermore, BMPs are known to induce the condensation of MSCs when administered *in vivo*[17–19].

Inorganic biomaterials, such as carbon fibers[20], collagen scaffolds[2,21], absorbable polymers[22,23], and hydroxyapatite[24,25], have been used for articular cartilage repair. Some success has been achieved in the repair of small osteochondral defects, but no widely accepted method exists for the complete healing of hyaline cartilage. The cause of the failure lies not in the nature of the biomaterial itself but in its structure, which is not regulated three-dimensionally.

In the present study, we attempted to combine two distinct approaches: the strong induction of subchondral bone regeneration, with a view to recruiting bone-marrow MSCs to the osteochondral defect; and the appropriate local delivery of rhBMP-2 to induce chondrocytic differentiation and to stimulate matrix production by the chondrocytes. To instigate these two approaches simultaneously, we developed a combined biomaterial, which consists of a synthetic hydroxyapatite with an interconnected porous structure (IP-CHA), and a synthetic bioabsorbable polymer, namely, PLA–PEG (poly-D,L-lactic acid–polyethylene glycol block copolymer). In this system, PLA–PEG serves as a drug-delivery carrier, which permits the ideal release of rhBMP-2 over a period of about 3 weeks[26–29]. IP-CHA is made from hydroxyapatite, which is a bioactive ceramic with osteoconductive properties[30,31]. In addition, IP-CHA has a finely organized, three-dimensional interconnecting pore structure. The material is highly porous (porosity: 75%) and the pore size (150 μm) is appropriate for bone formation. The large interconnecting channels (average diameter: 40 μm) permit the easy penetration of tissue into the deep pores[30]. Owing to these structural properties, IP-CHA can itself induce local bone repair processes[30,32,33]. The interconnecting pore structure of the material also permits its easy impregnation with cytokines or growth factors borne by an appropriate delivery system.

The rationale behind the selection of key experimental design parameters was as follows: Skeletally immature adolescent rabbits (4–6 months old and 2.5–3.0 kg in weight) were selected because the ability of articular cartilage to repair depends mostly on the bone-marrow MSCs, which are metabolically more active and have a higher capacity to induce repair in an immature model. The decision to use full-thickness defects with a diameter of 4 mm and a depth of 6 mm was based on the results of previous studies. In rabbits, partial-thickness defects do not heal spontaneously, whereas full-thickness ones with a diameter less than 3 mm do, and the repair tissue is composed either of hyaline- or of fibrocartilage[34–36]. Hence, it was necessary to establish a model in which this upper limit for spontaneous repair was exceeded.

In the present study, we demonstrate the capacity of the triple composite of rhBMP-2, PLA-PEG, and IP-CHA to effect articular cartilage repair. The goal was to achieve the repair of full-thickness articular cartilage defects in rabbits in as short a time as possible, with the ultimate view of inducing the repair of similar lesions in humans; specifically, those generated during osteoarthritis, rheumatoid arthritis, and osteochondritis dissecans.

Materials and methods

PREPARATION OF IMPLANTS

IP-CHA was synthesized by Toshiba Ceramics Co., Ltd. (Kanagawa, Japan), as previously described[30]. In short, we adopted a "foam gel" technique, which involves two unique steps: a foaming step and a crosslinking step. During the foaming step, the hydroxyapatite slurry is mixed with a foaming agent (polyethyleneimine, 40% by weight). During the crosslinking (polymerization) step, the foam-like hydroxyapatite slurry is rapidly gelatinized using a water-soluble crosslinking agent (a poly-functional epoxy compound)[30].

rhBMP-2, which is produced by the Genetics Institute (Cambridge, MA) and was given to us by Yamanouchi Pharmaceutical Co., Ltd. (Ibaraki, Japan), was dissolved in buffer (5 mM glutamic acid, 2.5% glycine, 0.5% sucrose, and 0.01% Tween 80) at a concentration of 1 mg/ml. The solution was then filter-sterilized. Two-hundred mg of PLA–PEG [molecular weight (MW) = 11,400, dispersity (Mw/Mn) = 1.1 (Taki Chemical Research Laboratory, Kanagawa, Japan)] was dissolved in 1 ml of acetone. To prepare a single implant sample, a 25 μl aliquot of the PLA–PEG mass (5 mg) was mixed with a 20 μl sample of rhBMP-2 (20 μg). The specimen of IP-CHA (4 mm in diameter and 4 mm in height) was immersed in the mixture and the solvent was evaporated in a centrifuge/evaporator. The resulting BMP/PLA–PEG/IP-CHA composite was sterilized with ethylene oxide gas for 24 h on the day preceding implantation.

IN VITRO RELEASE KINETICS OF RHBMP-2

The release of rhBMP-2 from the BMP/PLA–PEG/IP-CHA composite was measured using a quantitative sandwich enzyme immunoassay technique (AN'ALYZA®; BMP-2 immunoassay, TECHNE Co. MN, USA). The dose of rhBMP-2 used in the *in vivo* experiments (20 μg) was chosen for the release study. Twelve BMP/PLA–PEG/IP-CHA composites, which were prepared in the same way as those used for implantation in the rabbit model, were placed within 24-well plates together with 500 μl of phosphate-buffered saline [(PBS) Sigma] and incubated for 21 days at 37°C. The supernatant was removed and replaced with fresh PBS every day. The supernatants removed on days 1, 3, 7, 14 and 21 were analyzed for their concentrations of rhBMP-2 according to the enzyme-linked immunosorbent assay (ELISA) technique. The bioactivity of the composites maintained *in vitro* for 0, 7 and 21 days (four samples per time point) was also assessed (see next section).

IN VIVO BIOASSAY FOR THE BMP/PLA–PEG/IP-CHA COMPOSITE

To assess the biological activity of composites that were maintained *in vitro* for 0, 7 and 21 days, these, as well as

IP-CHAs without rhBMP-2 (controls), were implanted within the back muscles of 5-week-old male JCL: ICR mice (one composite per animal; four mice per group, i.e., control, day 1, day 7 and day 21) as previously reported[27,28]. The implants were harvested 2 weeks after implantation. They were then crushed, homogenized in 0.2% Nonidet P-40 containing 1 mM $MgCl_2$, and centrifuged at 10,000 rpm for 1 min at 4°C. The supernatants were assayed for alkaline phosphatase (ALP) activity using *p*-nitrophenyl phosphate as a substrate. The product was measured spectrophotometrically at an absorption wavelength of 410 nm ($n = 4$ per group)[37].

ANIMAL EXPERIMENTS

Fifty-two New Zealand White rabbits weighing 2.5–3.0 kg (4–6 months) were kept in cages and had free access to food pellets and water. The rabbits were anesthetized by the intravenous injection of 1 ml of pentobarbital [50 mg/ml (Nembutal®; Dainippon Pharmaceutical Co. Ltd., Osaka, Japan)] and the intramuscular injection of 1 ml of xylazine hydrochloride [25 mg/ml (Seractal®; Bayer, Germany)]. After shaving, disinfection, and draping, a straight 3-cm long medial parapatellar incision was made over the right knee and the patella was everted. Full-thickness articular osteochondral defects, 4 mm in diameter and 6 mm in depth, were created mechanically in the patellar groove of the right distal femur. Rabbit knees were divided into four implant groups: group I ($n = 16$ knees) received the BMP/PLA–PEG/IP-CHA composite; group II ($n = 12$ knees) received the PLA–PEG/IP-CHA composite (no rhBMP-2), group III ($n = 12$ knees) received IP-CHA alone; and group IV ($n = 12$ knees) underwent a sham operation with no implantation. In groups I, II, and III, all implants were placed at the subchondral bone level, 2 mm beneath the surface of the adjacent cartilage. The fascial layer was closed with absorbable sutures, and the skin with 4-0 nylon sutures. One week after surgery, four rabbits in group I were killed. At 3 weeks, 24 rabbits were killed (group I = 6, group II = 6, group III = 6, group IV = 6), and at 6 weeks 24 rabbits were killed (group I = 6, group II = 6, group III = 6, group IV = 6). The animals were killed by an intravenous injection of 5 ml of pentobarbital (Table I). All animal experiments were approved by the Animal Laboratory, Faculty of Medicine, Osaka University, Japan.

RADIOGRAPHIC AND HISTOLOGICAL EVALUATIONS

The harvested tissues were radiographed using a soft X-ray apparatus [35 kV; 300 μA; 300 s; MX20 (Faxitron X-ray Co., IL, USA)] and then fixed in 4% paraformaldehyde (pH 7.4) for 48 h at 4°C. Tissue samples were decalcified in 20% ethylenediaminetetraacetic acid (pH 7.4) at 4°C, dehydrated in a graded ethanol series and embedded in paraffin. Serial sections (5 μm in thickness) were cut sagittally through the center of the operative site and stained with hematoxylin and eosin (H&E) or with safranin-O. For the immunohistochemical analysis, paraffin sections were treated with 3% H_2O_2 to block endogenous peroxidase activity. They were pretreated with serum to block non-specific staining. The sections were then incubated with mouse monoclonal antibodies: anti-type-I collagen (I-8H5, Daiichi Fine Chemical Co., Ltd, Toyama, Japan), anti-type-II collagen (II-4C11, Daiichi Fine Chemical Co., Ltd, Toyama, Japan), and anti-CD105 [(Endoglin) 555722, BD Bioscience, NJ, USA]; and with the polyclonal antibody goat anti-Cbfa1 [(Runx2) C-19, Santa Cruz, CA, USA][38]. The specimens were treated with the appropriate biotinylated secondary antibodies, and then incubated with the streptavidin/horseradish peroxidase complex. The signal was visualized as the red reaction product of a 3-amino-9-ethyl carbazole liquid substrate chromogen (AEC, DAKO JAPAN Co., Ltd, Kyoto, Japan). To confirm the specificity of

Table I
Information respecting the deployment of the 52 rabbits used in this study

	Number of rabbits				Total number
	Group I	Group II	Group III	Group IV	
Materials					
IP-CHA	+	+	+	–	
rhBMP-2	+	–	–	–	
PLA–PEG	+	+	–	–	
Follow-up time					
1 week	4	0	0	0	4
3 weeks	6	6	6	6	24
6 weeks	6	6	6	6	24
Total number	16	12	12	12	52

Table II
*Histological scoring system**

Category	Points
Cell morphology	
Hyaline cartilage	4
Mostly hyaline cartilage	3
Mostly fibrocartilage	2
Mostly non-cartilage	1
Non-cartilage only	0
Matrix-staining (metachromasia)	
Normal	3
Slightly reduced	2
Markedly reduced	1
No metachromatic staining	0
Structural integrity	
Normal	2
Slight disruption	1
Severe disintegration	0
Surface regularity†	
Smooth	3
Moderate	2
Irregular	1
Severely irregular	0
Thickness of cartilage, %	
121–150	1
81–120	2
51–80	1
0–50	0
Regenerated subchondral bone	
Good	2
Moderate	1
Poor	0
Integration with adjacent cartilage	
Both edges integrated	2
One edge integrated	1
Neither edge integrated	0
Total maximum	18

*A modified version of the system described by Wakitani *et al.*[8].

†Total smooth area of repair cartilage compared with the entire area of the cartilaginous compartment of the defect.

the antibody under the adopted conditions and to confirm the specificity of the markers in target cells, all antibodies were tested for their reactivity in control tissues.

HISTOLOGICAL SCORING

To quantify the histological repair of articular cartilage defects, we employed a modified version of the grading scale described by Wakitani *et al.*[8]. This consists of seven categories and assigns a score ranging from 0 to 18 points (Table II). The following parameters were assessed: cell morphology (hyaline cartilage); metachromatic staining of the cartilage matrix; structural integrity of the regenerated cartilage; surface regularity of the tissue; thickness of the cartilage layer; regeneration of the subchondral bone; and integration of the tissue with adjacent cartilage.

STATISTICAL ANALYSES

Data pertaining to ALP activity were analyzed using an unpaired Student's *t* test. The histological scoring data were analyzed using the Kruskal–Wallis test, with a *post hoc* Bonferroni correction for non-parametric data.

Results

EVALUATION OF THE IMPLANTS

Scanning electron microscopy of IP-CHA samples revealed these to have a finely organized three-dimensional structure. Most of the IP-CHA pores were spherical, of similar size (approximately 100–200 μm in diameter) and uniformly interconnected via channels [10–80 μm in diameter; Fig. 1(B, C)]. Scanning electron microscopy of the BMP/PLA–PEG/IP-CHA composite revealed the BMP/PLA–PEG component to affect neither the pore size nor the interconnecting pore structure and to coat well the surface of the IP-CHA [Fig. 1(D, E)].

IN VITRO RELEASE KINETICS OF RHBMP-2 AND *IN VIVO* BIOASSAY FOR THE BMP/PLA–PEG/IP-CHA COMPOSITE

Based on ELISA, the BMP/PLA–PEG/IP-CHA composite released significant quantities of rhBMP-2 during the 21-day monitoring period [6.85 ± 1.31 μg/ml on day 1, 0.79 ± 0.22 μg/ml on day 3, 22.9 ± 0.62 ng/ml on day 7, 4.76 ± 1.13 ng/ml on day 14, and 2.71 ± 0.70 ng/ml on day 21; Fig. 2(A)].

To assess the bioactivity of the BMP/PLA–PEG/IP-CHA composites maintained *in vitro* for 0, 7 or 21 days, we implanted these, as well as IP-CHAs (control for the absence of rhBMP-2) within the back muscles of male ICR mice (a standard ectopic bone-formation model) and then analyzed the explanted material for its ALP activity. High levels of ALP activity could be detected even on day 21 [Fig. 2(B)], which accords with the rhBMP-2 release kinetics results *in vitro*.

MACROSCOPIC OBSERVATIONS OF CARTILAGE DEFECTS

Three weeks after implantation, the repaired defects in group I had a macroscopically smooth and glistening appearance and exhibited continuity with the surrounding host cartilage [Fig. 3(A)]. The controls (groups II–IV) revealed varying degrees of cartilage resurfacing with fibrous tissue [Fig. 3(B–D)].

At 6 weeks, the color and the glistening appearance of the repaired defects in group I were similar to those manifested by the adjacent host cartilage. The junction between the repaired tissue and the surrounding host cartilage was not clearly visible [Fig. 3(E)]. In contrast, the regenerated tissue in the control groups (groups II–IV) was

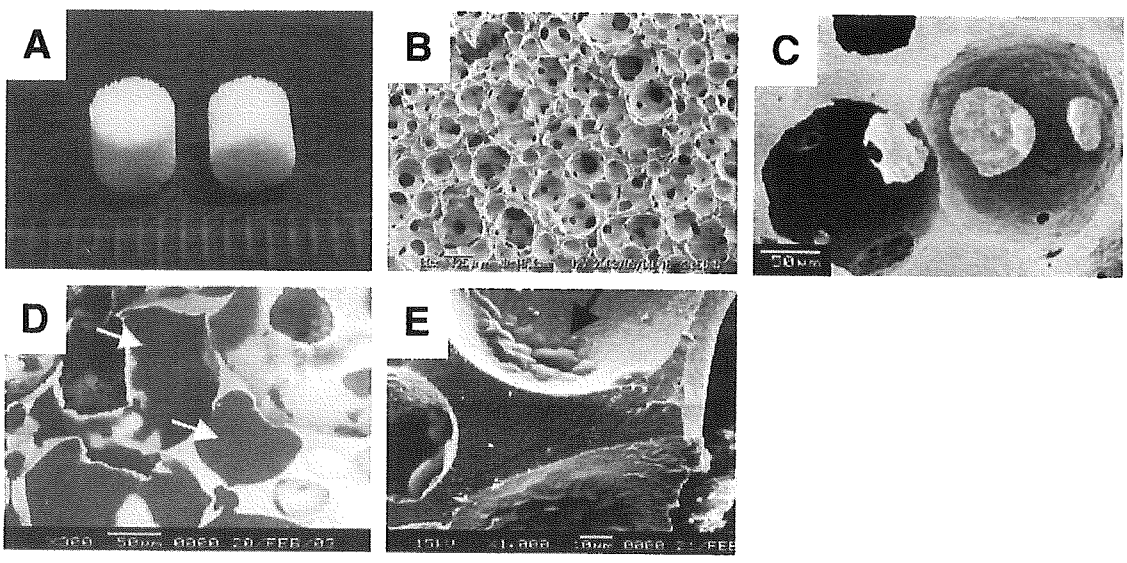

Fig. 1. Macroscopic photograph (A) and scanning electron micrographs (B–E) of IP-CHA specimens (4 mm in diameter and 4 mm in height). (A) Macroscopically, the surface of IP-CHA is slightly rough compared with that of other commercial porous hydroxyapatite materials, owing to its regular porous structure. (B, C) Scanning electron micrographs of IP-CHA, illustrating the regular arrangement of pores which are of similar size (100–200 μm in diameter), uniformly connected with each other, and separated by thin walls. (B) = 80×; (C) = 600×. (D, E) Scanning electron micrographs of the BMP/PLA–PEG/IP-CHA composite. (D) The dark areas lining the pores (white arrows) represent the BMP/PLA–PEG component. The introduction of BMP/PLA–PEG had no effect on either the pore size or the interconnecting pore structure. (E) Higher magnification of the lining of a pore (black arrow), revealing it to be well coated with BMP/PLA–PEG. (D) = 300×; (E) = 1000×.

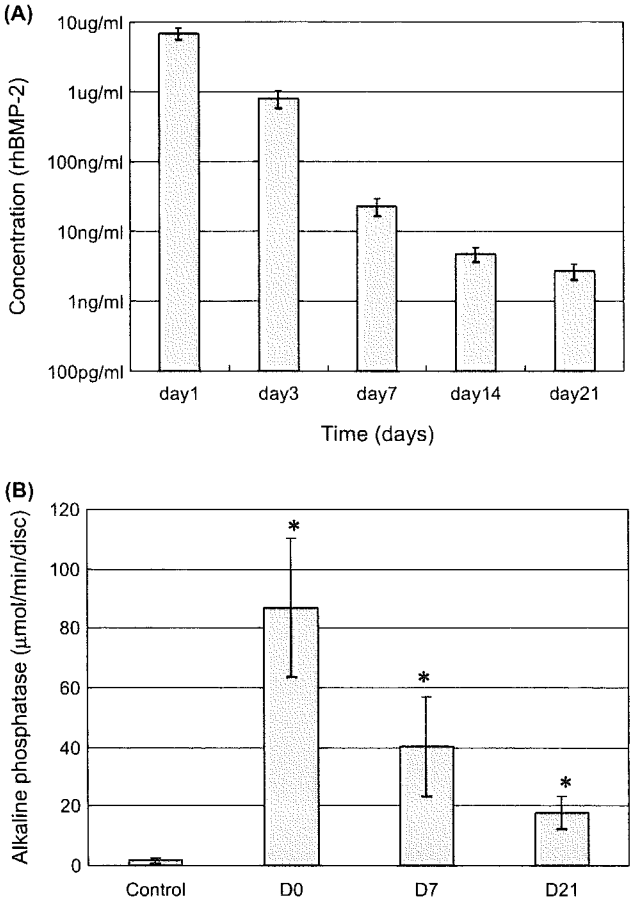

Fig. 2. Time course of rhBMP-2 release from the BMP/PLA–PEG/IP-CHA composite *in vitro* (A) and the bioactivity of the composites *in vivo* (B). (A) Release kinetics (measured by ELISA) of rhBMP-2 from the BMP/PLA–PEG/IP-CHA composite, illustrating significant quantities of rhBMP-2 during the 21-day monitoring period. The bar graph depicts the non-cumulative release at each time point. Mean values ± SD ($n = 4$) are represented. (B) The bioactivity of BMP/PLA–PEG/IP-CHA composites that were maintained *in vitro* for 0 (D0), 7 (D7), or 21 (D21) days was assessed 2 weeks after their implantation at an ectopic site in mice by monitoring the ALP activity of the explanted material. PLA–PEG/IP-CHA (no rhBMP-2) represented the control. High levels of ALP activity could be detected even on day 21 [86.8 ± 23.2 μmol/min/disc (day 0), 40.3 ± 16.8 μmol/min/disc (day 7), 17.7 ± 5.2 μmol/min/disc (day 21), 1.6 ± 0.8 μmol/min/disc (control)]. Mean values ± SD ($n = 4$) are represented. * = value is significantly different from the control ($P < 0.05$).

fibrous, and had a rough surface containing many fissures [Fig. 3(F–H)].

RADIOGRAPHIC EVALUATION

Six weeks after implantation, the soft X-ray analysis revealed defects treated with the BMP/PLA–PEG/IP-CHA composite (group I) to be consistently filled with newly formed bone, which was continuous with the surrounding intact subchondral bone [Fig. 3(I)]. In the control groups (groups II–IV), bone formation was incomplete and irregular [Fig. 3(J–L)].

HISTOLOGICAL EVALUATION

One week after implantation with the BMP/PLA–PEG/IP-CHA composite (group I), vigorous new bone formation was observed histologically within the pores of the IP-CHA scaffold [Fig. 4(B)], and about three-quarters of the defect depth above the IP-CHA had already been replaced with repair tissue. The central part of the repair tissue contained a fibrin clot and a few vessels. The lateral and lower regions consisted of granulation tissue, which was actively undergoing neovascularization and contained rounded fibroblast-like cells. These cells registered positive for Cbfa1 and/or CD105. They appeared to have infiltrated from the surrounding intact subchondral bone, either directly, or indirectly via the interconnecting IP-CHA pores, which were likewise filled with granulation tissue. Some of the pores in the peripheral 1-mm portions of IP-CHA blocks already contained newly formed bone (Fig. 4).

Three weeks after implantation with BMP/PLA–PEG/IP-CHA, the defect space above the IP-CHA blocks (subchondral space) was filled with newly generated and vigorous bone tissue, which penetrated the interconnecting pores of this material [Fig. 5(A, F)]. The regenerated articular cartilage was more cellular and contained less extracellular matrix than normal cartilage. The regenerated cartilage was divided into three distinct zones: (1) a superficial one, which contained flattened hyperchromatic cells; (2) a middle one, which contained rounded chondrocytes; and (3) a zone of enchondral ossification. The cartilage-like layer was two-to-three times thicker than normal cartilage [Fig. 5(A, E)]. In each of the control groups (groups II–IV), the regenerated fibrous cartilage had a similar morphological appearance, irrespective of the absence or presence of an implant. Although the subchondral space in group II tended to be filled with more newly formed bone than did that in the other control groups (groups III and IV), the quantitative histological evaluation revealed no significant difference between them [Table III; Fig. 5(B–D)].

Six weeks after implantation, defects treated with the BMP/PLA–PEG/IP-CHA composite (group I) were filled with regenerated subchondral bone, which also penetrated the pores of the implant. The subchondral bone was covered with a layer of regenerated cartilage tissue of almost normal thickness. The hyaline nature of the cartilage was maintained, and the tissue was beginning to assume a columnar organization and a horizontal stratification into four distinct zones (superficial, middle, deep and calcified), as in normal cartilage [Fig. 6(A, E)]. Interestingly, no gaps could be distinguished microscopically between the host cartilage and the newly regenerated cartilage, which suggests that the tissues were functionally and biologically integrated [Fig. 6(F)]. Safranin-O staining was evident predominantly in the middle and deep zones. Immunoreactivity for type-II collagen tended to be weakest in the deep zone at the junction with host tissue. But generally, the matrix exhibited a hyaline-like cartilaginous phenotype [registering negative for type-I collagen; Fig. 6(J–L)]. In contrast, defects in the control groups (groups II–IV) were filled with a hypercellular type of fibrous tissue. No hyaline cartilage was detected, despite the presence of new bone above and within the implant; [Fig. 6(B–D, G–I)]. Histological sections were assessed quantitatively using a modified version of an established grading system, which measures the degree and quality of cartilage repair[8] (Table II). At each time point, the scores for the BMP/PLA–PEG/IP-CHA composite (group I) were significantly better than those for groups II, III and IV ($P < 0.01$). These findings accord with the macroscopic and histological observations.

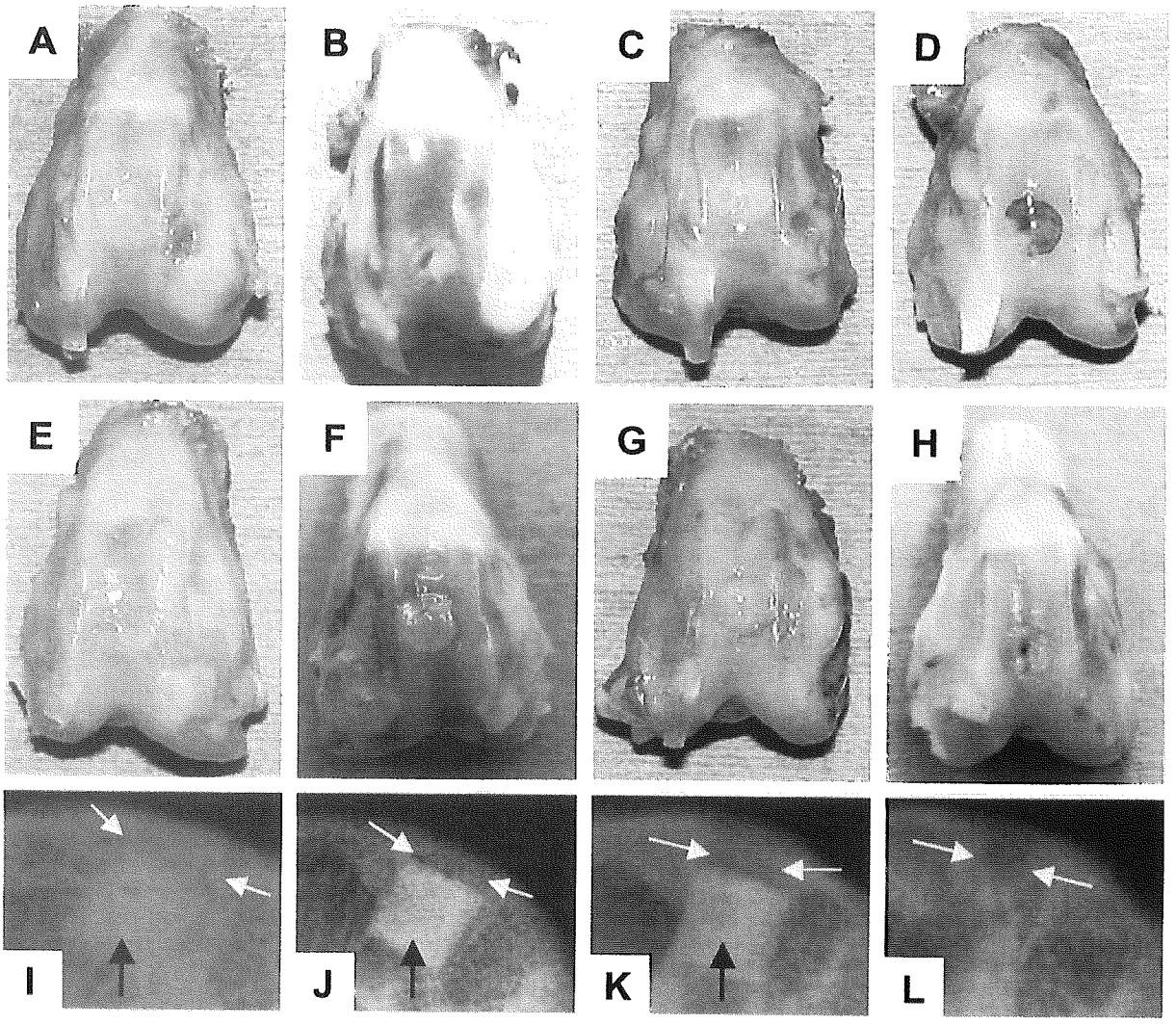

Fig. 3. Gross appearance (A–H) and soft X-ray photographs (I–L) of four specimens (one in each group) 3 weeks (A–D) and 6 weeks (E–L) after implantation. (A, E, I): BMP/PLA–PEG/IP-CHA composite (group I). (B, F, J): PLA–PEG/IP-CHA composite (group II). (C, G, K): IP-CHA alone (group III). (D, H, L): no implant (group IV). (A, E) In group I, reconstruction of the surface was good. At 3 weeks, the surface was still a little "white"; but at 6 weeks, it was smooth and glistening and exhibited continuity with the surrounding intact host cartilage. These macroscopic findings correspond with the histological results (Table III). (B, F) In group II, the articular cartilage defects were covered with "white" fibrous tissue with many fissures. (C, G) In group III, the regeneration of the defect looked better than those of other control groups (group II and IV), whereas the junction of the defects were still visible. (D, H) In group IV, in which the defects were left empty, at 3 weeks the defects were filled with red, semitransparent tissue with the margins sharply defined and the edges completely discernible (D). At 6 weeks, the defects were filled with irregular "white" tissue with pin-hole like fissure (H). (I–L) Representative soft X-ray photographs of the four specimens. The black arrows denote the implanted IP-CHA block. The white arrows above the IP-CHA block indicate the region where subchondral bone should be regenerated. A white, radiodense zone was observed above the IP-CHA block in group I (I); it denotes a vigorous regeneration of subchondral bone. This radiodense zone was not detected in groups II–IV (J–L).

Discussion

Several investigators have reported on the repair of articular cartilage defects using diverse tissue-engineering approaches. These include a gene-enhanced technique, the direct implantation of growth factors, and *in vitro* cell expansion[39–42]. BMPs have been shown to induce the differentiation of MSCs into chondrocytes both *in vitro* and *in vivo*. BMPs (BMP-2 and BMP-7) have also been used in conjunction with type-I collagen sponges to elicit the repair of osteochondral defects[43–45]. Cook *et al.*[40] have reported that type-I collagen sponges impregnated with rhBMP-7 can induce the repair of full-thickness osteochondral defects with hyaline-like cartilage in a dog model. The hyaline-like quality of the repair cartilage was still evident 52 weeks after surgery and the tissue had undergone no significant degradation. Sellers *et al.*[41] have demonstrated the capacity of rhBMP-2 to accelerate the healing of full-thickness articular cartilage defects and to improve the histological appearance and the biochemical characteristics of the repair cartilage. However, the tissue still differed from normal hyaline cartilage, both biochemically and structurally, and a long time elapsed before the defect area was completely filled with it. These suboptimal results probably reflect a limited recruitment of MSCs and/or a restricted delivery of cytokines, owing to the poor structural

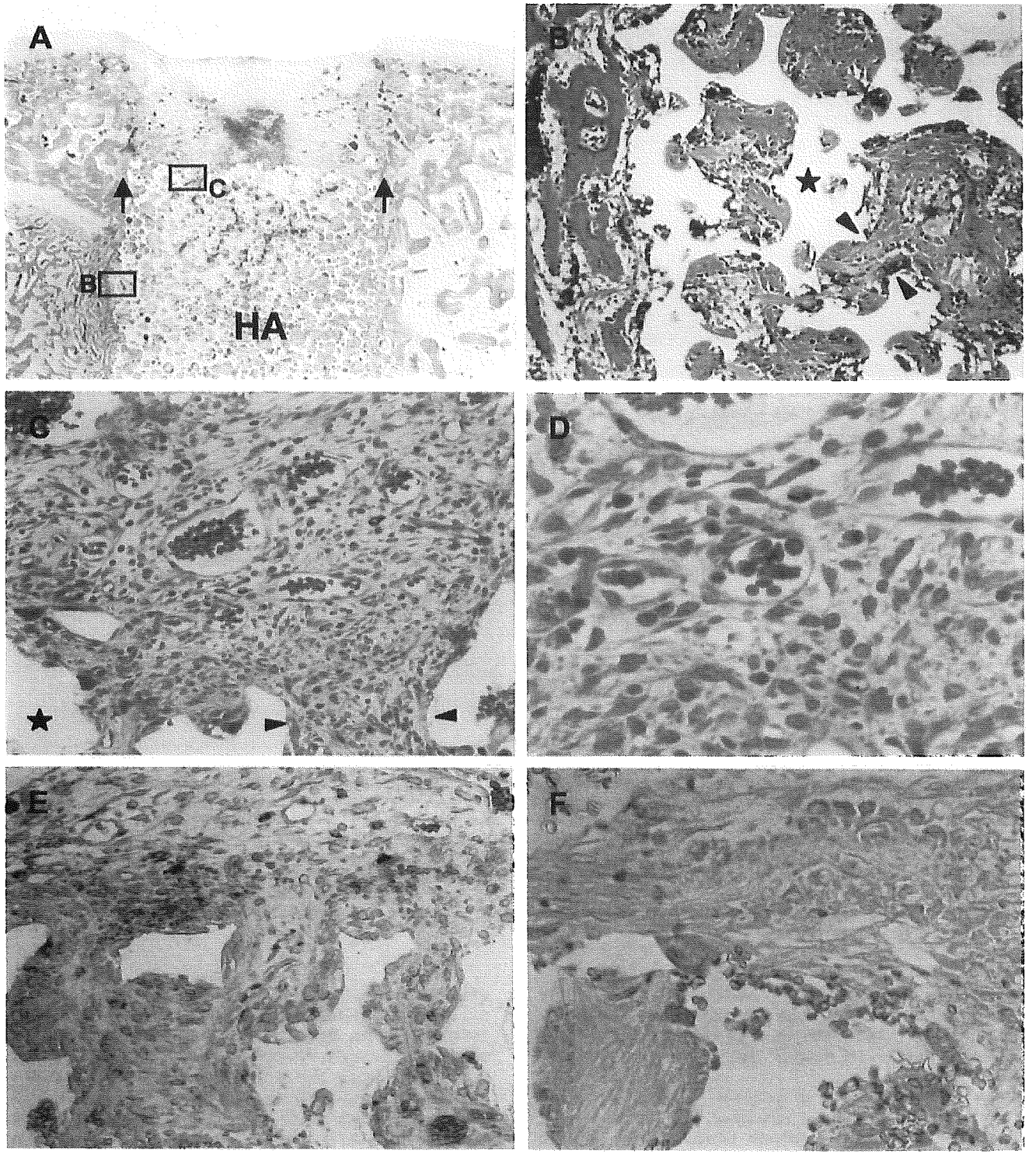

Fig. 4. Histological photomicrographs of a defect 1 week after the implantation of a BMP/PLA–PEG/IP-CHA composite (group I). (A) Overview of the defect site, the margins of which are indicated by arrows. HA represents the implanted IP-CHA scaffold (H&E). (B) Higher magnification of the region indicated in (A). The surface of newly formed bone trabeculae are lined with numerous cuboidal osteoblasts which have migrated from the neighboring host bone. (C) Higher magnification of the region indicated in (A), illustrating a neovascularized aggregate of cells which have migrated from the neighboring bone marrow, either directly or indirectly via the interconnecting channels of the IP-CHA composite. The arrowheads in (B) and (C) indicate the interconnecting pores of the IP-CHA scaffold. The asterisks denote regions that were occupied by hydroxyapatite before decalcification. (D) Higher magnification of (C), illustrating the rounded, fibroblast-like form of the aggregated cells. (E, F) Immunostaining of the aggregated cells for Cbfa1 (E) and CD105 (F). Many of the cells expressed the chondro/osteoblastic marker (E) and/or the mesenchymal one (F). Magnification: (A) = 10×; (B, C) = 100×; (E, F) = 200×; (D) = 400×.

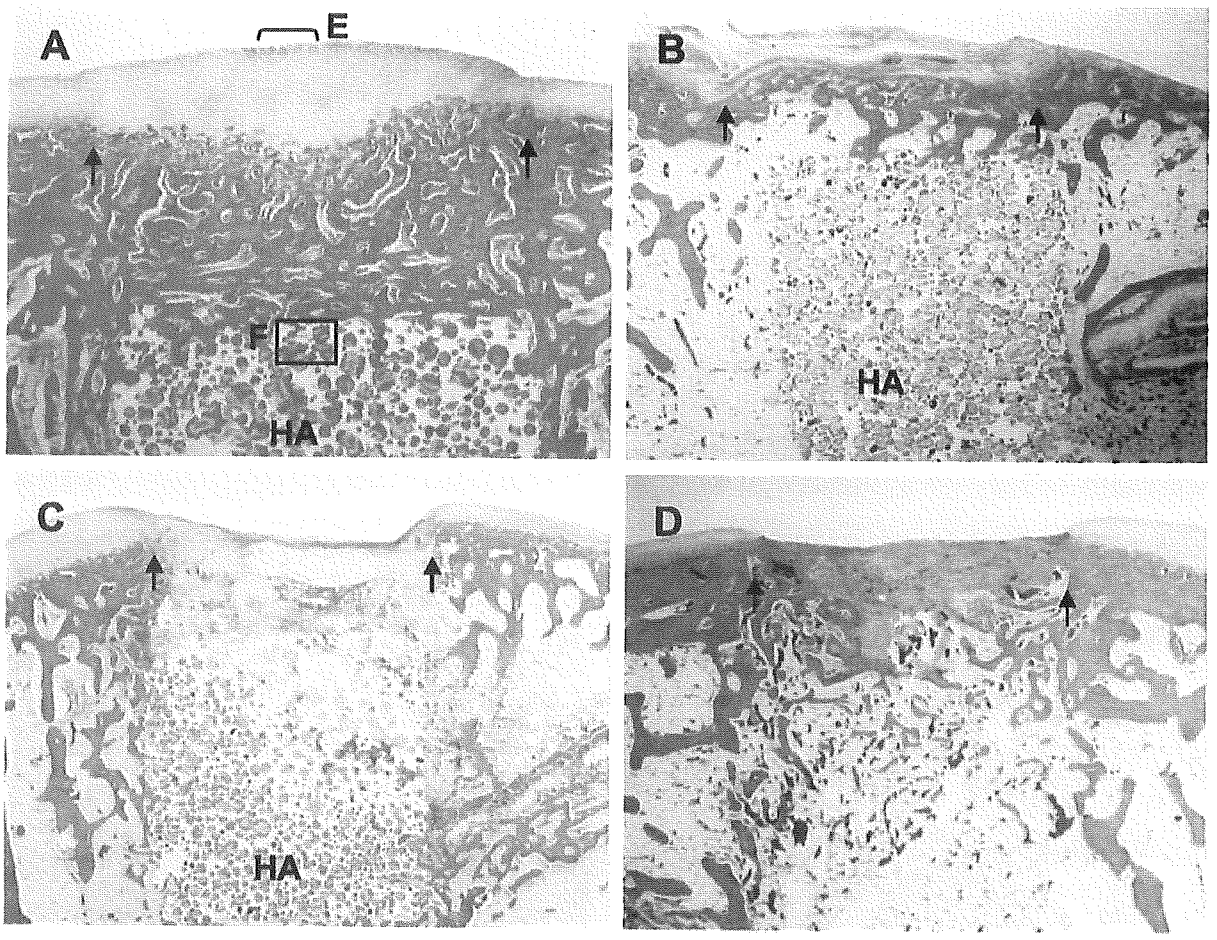

Fig. 5. Histological photomicrographs of defects (H&E staining) 3 weeks after implantation with either the BMP/PLA–PEG/IP-CHA composite [(group I) A, E, F], the PLA–PEG/IP-CHA composite [(group II) B], or IP-CHA alone [(group III) C], and in the absence of treatment [empty (group IV) D]. Arrows indicate the margins of the defect. HA represents the implanted IP-CHA scaffold. Highly magnified images of the regions indicated in (A) are represented in (E) and (F). (A) Section of a defect filled with the BMP/PLA–PEG/IP-CHA composite (group I), illustrating well-organized hyaline-like cartilage and accelerated replacement of vigorous subchondral bone. (B–D) In each of the control groups (group II–IV), the regenerated tissue had a similar morphological appearance, irrespective of the absence or presence of an implant. The defect site was filled predominantly with a hypocellular fibrocartilage repair tissue with incomplete replacement of subchondral bone. (E) The regenerated articular cartilage was more cellular and contained less extracellular matrix than normal cartilage. However, a stratified structure similar to normal cartilage was already visible. (F) Vigorous regeneration of subchondral bone occurred, which was carried up through the interconnections of the IP-CHA scaffold (arrowheads). The asterisk denotes a region that was occupied by hydroxyapatite before decalcification. Magnification: (A–D) = 10×; (E, F) = 100×.

organization of the supporting scaffold. The purpose of the present study was to evaluate the potential of IP-CHA to serve as a scaffold for the repair of full-thickness articular cartilage defects. This material has a well-organized interpore connectivity.

The osteoconductivity of polymer implants containing rhBMP-2 has been studied extensively[28,46]. In the present study, we used the synthetic bioabsorbable polymer PLA–PEG as a carrier for rhBMP-2. *In vitro*, rhBMP-2 was released continuously from the BMP/PLA–PEG/IP-CHA composite over a period of 21 days, as determined by ELISA [Fig. 2(A)]. This finding accords with the results of the *in vivo* bioassay [Fig. 2(B)], which was based on the ALP activity of composites implanted at an ectopic site in mice. However, it is of course conceivable that the release profile of rhBMP-2 at this ectopic site in mice differs greatly from that at the orthotopic site in our rabbit model.

Our new strategy for articular cartilage repair appears to be unique in three respects: (1) autogenous MSCs were efficiently recruited from the bone marrow by strongly activating regeneration within the subchondral bone compartment of the defect; (2) a sustained BMP stimulus appears to promote not only the vigorous regeneration of subchondral bone but also the ensuing differentiation of chondrocytes and the production of a cartilaginous matrix at the surface, which results in the regeneration of a hyaline-like cartilage layer in as short a time as 3 weeks; and (3) the regenerated cartilage integrated almost perfectly with the surrounding host cartilage, probably because the entire regeneration process was conducted *in situ*, i.e., it did not involve an *in vitro* chondrocyte-culturing step.

It is not known why the thickness of the repaired articular cartilage corresponded so closely to that of the host articular cartilage, with no bony differentiation. But articular factors, such as oxygen tension, joint effusion and mechanical stress, as well as subchondral influences, may regulate the differentiation process. Although the regenerated cartilage present 6 weeks after surgery was

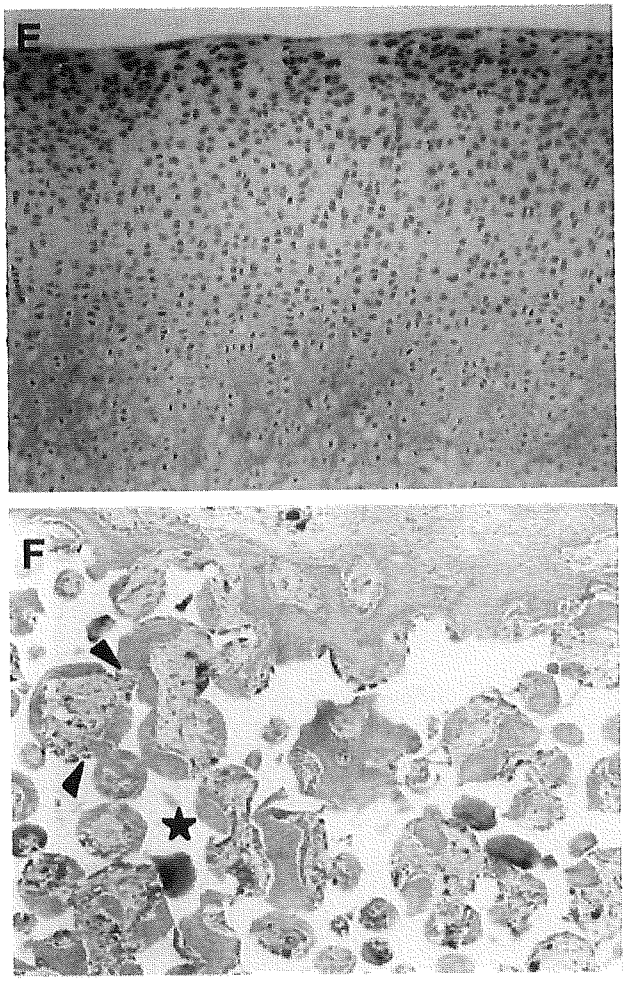

Fig. 5. (*continued*).

microscopically so well integrated with the surrounding host cartilage, the histological analysis revealed a slight discrepancy between safranin-O staining and immunoreactivity for type-II collagen [Fig. 6(J, L)]. This may be accounted for by the fact that chondrocytes near the junction with host cartilage produced less matrix than did those located more centrally within the regenerated tissue, where staining with safranin-O was absent only from the superficial zone, as in normal articular cartilage.

Cbfa1, a member of the Runt-domain family of transcriptional factors, is expressed not only in all osteoblasts, but also in chondrocytes and in earlier prechondrogenic mesenchymal condensations[47–49]. Furthermore, Cbfa1 is known to play an essential role in the differentiation not only of osteoblasts but also of chondrocytes, both at an early and a later stage of the process[50,51]. CD105 is a putative cell-surface marker for MSCs, which have the ability to undergo chondrogenesis, osteogenesis and adipogenesis[52,53]. One week after implantation, numerous cuboidal osteoblasts migrated into the pores of the IP-CHA scaffold from the host bone marrow (Fig. 3). And within peripheral pores, they had already begun to form bone tissue. The subchondral space above the IP-CHA scaffold was filled with an agglomeration of rounded fibroblast-like cells, which registered positive for Cbfa1 and/or CD105. They appeared to have migrated from the adjacent bone marrow, either directly, or indirectly via the interconnecting pores of the IP-CHA. These findings suggest that the aggregating fibroblast-like cells might have the potential for chondro/osteogenesis.

According to our findings, one of the keys to successful articular cartilage regeneration might be the activation of a subchondral repair process, thereby enabling chondroblastic/osteoblastic cells to effectively aggregate within the subchondral space. In rabbits, small, 3-mm-diameter, full-thickness articular cartilage defects heal spontaneously with repair tissue, which is composed of hyaline-like or fibrous cartilage. In adolescent rabbits (approximately 3 months old), osteochondral defects repair better and more rapidly than do those in adults[34,54]. Furthermore, adolescent rabbits have a larger population of metabolically active bone-marrow MSCs. Hence, in the present study, we established a large (4-mm-diameter) full-thickness defect model, it being necessary to exceed the upper limit (3 mm in diameter) for spontaneous repair. And since our system involved no cell-expansion step *in vitro*, the adolescent (rather than the adult) rabbit model was considered to be advantageous in its possession of a larger population of metabolically active bone-marrow MSCs.

A basic requirement for biomaterials is that they be non-carcinogenic and elicit no inflammatory reaction due to cytotoxicity or immunogenicity[55]. The BMP/PLA–PEG/IP-CHA composite is believed to meet these criteria. The PLA and PEG homopolymers and hydroxyapatite have been shown to be compatible and safe for clinical applications[30,56]. In addition to these safety features, it is crucial that biomaterials are easy to handle in clinical settings.

Table III
Results of the histological scoring

Group	No. of defects	Cell morphology	Matrix-staining	Structural integrity	Surface regularity	Thickness	Reconstruction of subchondral bone	Integration with adjacent cartilage	Total score
Group I: 3 weeks	6	3.6 ± 0.5*	2.0 ± 0	1.3 ± 0.5	2.0 ± 0.9	1.2 ± 0.4	0.8 ± 0.7	1.8 ± 0.4§	12.8 ± 2.4*
Group II: 3 weeks	6	1.7 ± 0.5	1.0 ± 0.6	0.5 ± 0.5	0.5 ± 0.5	0.7 ± 0.5	0.5 ± 0.4	1.0 ± 0.6§	5.8 ± 2.6
Group III: 3 weeks	6	2.2 ± 0.8	1.3 ± 0.5	0.5 ± 0.5	0.7 ± 0.4	1.0 ± 0	0.5 ± 0.4	1.2 ± 0.8§	7.2 ± 2.2
Group IV: 3 weeks	6	1.3 ± 0.5	0.8 ± 0.4	0.7 ± 0.5	1.3 ± 0.5	0.5 ± 0.3	0.5 ± 0.3	0.5 ± 0.3	5.1 ± 1.1
Group I: 6 weeks	6	3.8 ± 0.4*	2.3 ± 0.5*	1.5 ± 0.5§	2.2 ± 1.0	1.2 ± 0.4§	1.8 ± 0.4§	1.5 ± 0.5	15.0 ± 2.1*
Group II: 6 weeks	6	1.8 ± 0.4	1.5 ± 0.5	1.2 ± 0.4	1.5 ± 0.5	1.2 ± 0.4	1.3 ± 0.5§	1.2 ± 0.4	9.7 ± 1.2
Group III: 6 weeks	6	1.7 ± 1.0	1.0 ± 0.8	0.8 ± 0.4	1.7 ± 0.5	0.7 ± 0.5	1.3 ± 0.5§	1.2 ± 0.4	8.3 ± 3.0
Group IV: 6 weeks	6	1.5 ± 0.5	0.5 ± 0.4	0.5 ± 0.5	1.3 ± 0.5	0.7 ± 0.5	0.5 ± 0.3	0.8 ± 0.4	5.7 ± 1.9

Values represent the average score ± SD for each category. *$P < 0.01$ vs groups II, III, and IV. §$P < 0.01$ vs group IV.

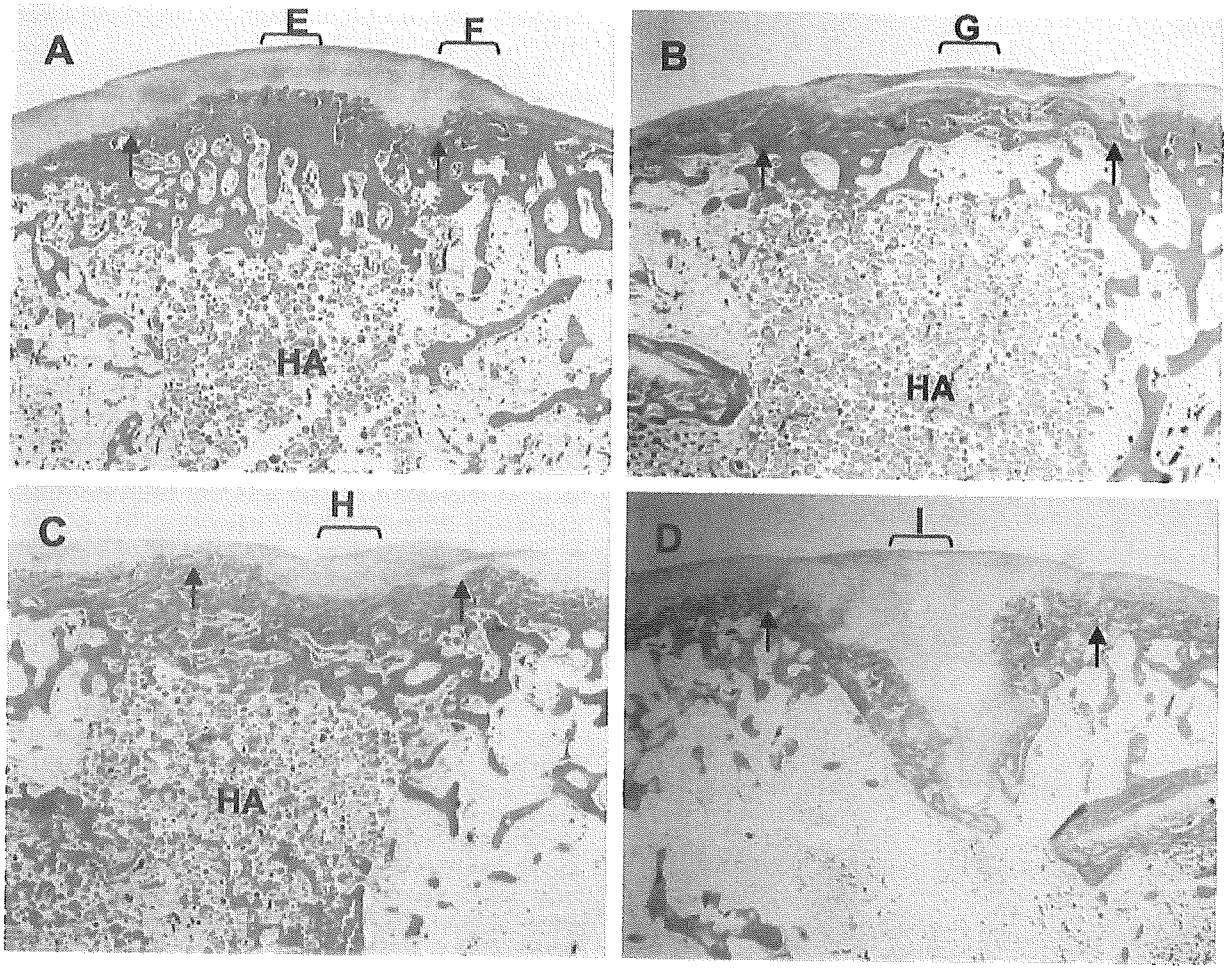

Fig. 6. Histological photomicrographs of defects 6 weeks after implantation with either the BMP/PLA–PEG/IP-CHA composite [(group I) A, E, F, J–L], the PLA–PEG/IP-CHA composite [(group II) B, G], or IP-CHA alone [(group III) C, H], and in the absence of treatment [empty (group IV) D, I]. Arrows indicate the margins of the defect. HA represents the implanted IP-CHA scaffold. Highly magnified images of the regions indicated in (A–D) are represented in (E–I). (A) The defect treated with the BMP/PLA–PEG/IP-CHA composite (group I) was filled with regenerated subchondral bone, which also penetrated the pores of the implant. The subchondral bone was covered with a layer of regenerated cartilage tissue of almost normal thickness. (B, C) In the control groups (group II and III), the defects were filled with a hypercellular type of fibrous tissue with regeneration of subchondral bone. The surface the repaired tissue was rough. (D) Without treatment (group IV), the defect site was predominantly replaced by thick fibrocartilage tissue with a thin layer of irregular subchondral bone. (E) The central region of the regenerated articular cartilage layer (group I). The repaired tissue has a hyaline-like appearance and is undergoing organization into vertical columns. The four horizontal strata characteristic of normal articular cartilage are apparent. (F) The junction between host and regenerated cartilage is continuous, and very little fibrillation of the articular surface is apparent (group I). (G–I) The repaired tissue is mainly of a fibrous nature (group II–IV). (J–L) Safranin-O staining (J), and immunostaining for type-I collagen (K) and type-II collagen (L) at the junction between host and the regenerated cartilage (group I). Magnification: (A–D) = 10×; (E–I) = 100×; (J–L) = 40×. (A–I): H&E staining.

Current techniques using cultured chondrocyte suspensions or collagen gels are complicated by problems associated with cell retention. Our composite material circumvents these problems. Furthermore, our material may be shaped into a "ready-to-use" form. It is possible to adjust its size and shape to suit the dimensions of the defect prior to implantation.

In conclusion, we have successfully induced the repair of articular cartilage defects within a relatively short period of time by combining rhBMP-2 with two biomaterials: IP-CHA as a scaffold and PLA–PEG as a carrier for rhBMP-2. The BMP/PLA–PEG/IP-CHA composite represents a new and promising technology for the engineering of articular cartilage. Clinical applications for the treatment of both osteoarthritis and articular cartilage injuries are also anticipated. Further studies involving long-term observations in both adolescent and adult animals are currently underway.

Acknowledgments

The authors thank Toshiba Ceramics Co., Ltd. for supplying the materials used in this study and for their technical assistance. We also thank Miss K. Asai for her technical assistance. This study was partially supported by grants from the Japanese Ministry of Health and Welfare, the Japanese Ministry of Education, Science and Culture, the Uehara Memorial Foundation, the New Energy and

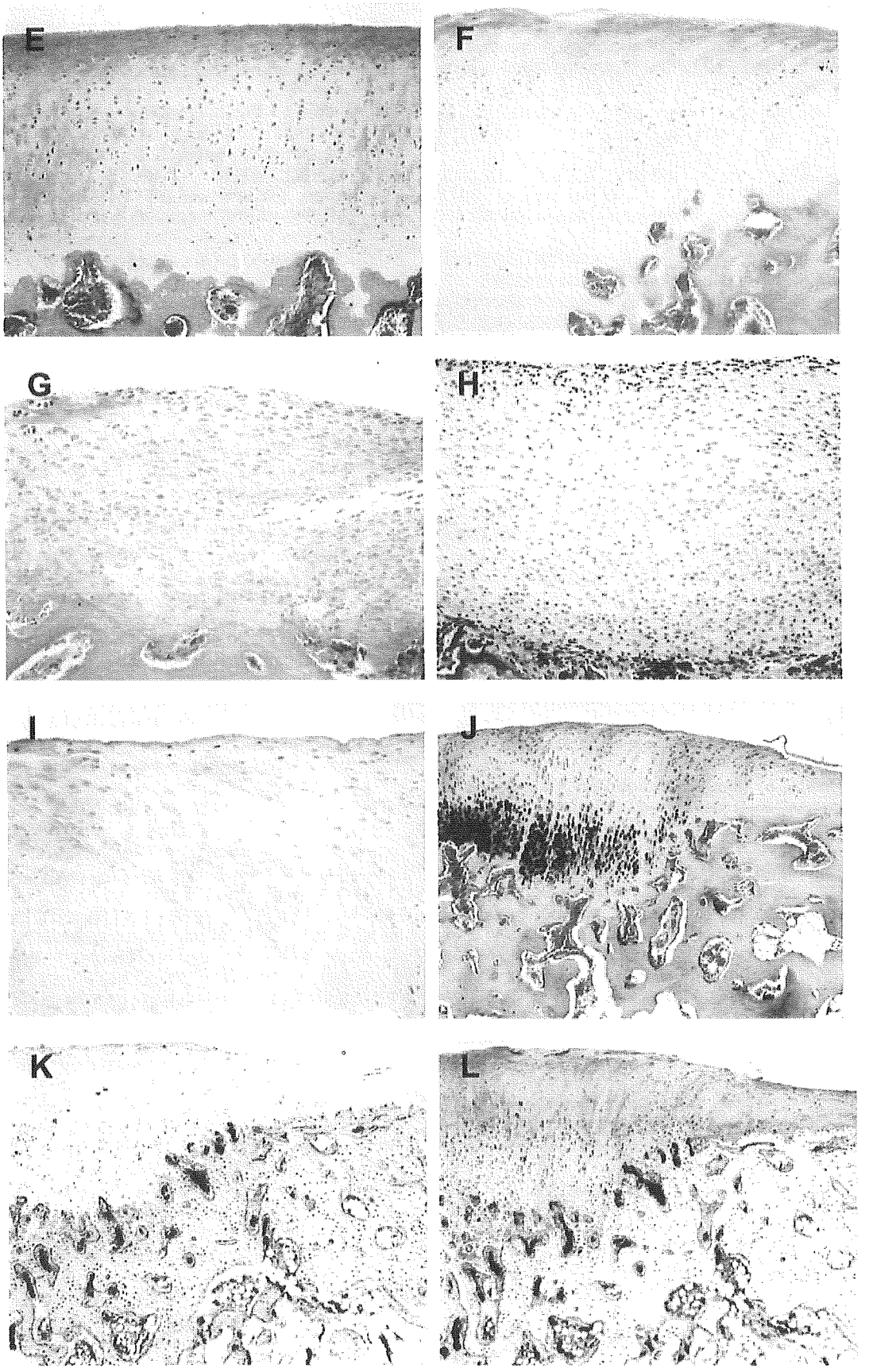

Fig. 6. (*continued*).

Industrial Technology Development Organization, the Japan Orthopaedics and Traumatology Foundation (No.0122), and JSPS Research Fellowships for Young Scientists (No. 04920).

References

1. Newman AP. Articular cartilage repair. Am J Sports Med 1998;26:309–24.
2. Lee CR, Grodzinsky AJ, Hsu HP, Spector M. Effects of a cultured autologous chondrocyte-seeded type II collagen scaffold on the healing of a chondral defect in a canine model. J Orthop Res 2003;21:272–81.
3. van Susante JL, Buma P, Homminga GN, van den Berg WB, Veth RP. Chondrocyte-seeded hydroxyapatite for repair of large articular cartilage defects. A pilot study in the goat. Biomaterials 1998;19:2367–74.
4. Mainil-Varlet P, Rieser F, Grogan S, Mueller W, Saager C, Jakob RP. Articular cartilage repair using a tissue-engineered cartilage-like implant: an animal study. Osteoarthritis Cartilage 2001;9:S6–S15.
5. Litzke LE, Wagner E, Baumgaertner W, Hetzel U, Josimovic-Alasevic O, Libera J. Repair of extensive articular cartilage defects in horses by autologous chondrocyte transplantation. Ann Biomed Eng 2004; 32:57–69.
6. Pittenger MF, Mackay AM, Beck SC, Jaiswal RK, Douglas R, Mosca JD, *et al.* Multilineage potential of adult human mesenchymal stem cells. Science 1999; 284:143–7.
7. Kadiyala S, Young RG, Thiede MA, Bruder SP. Culture expanded canine mesenchymal stem cells possess osteochondrogenic potential *in vivo* and *in vitro*. Cell Transplant 1997;6:125–34.
8. Wakitani S, Goto T, Pineda SJ, Young RG, Mansour JM, Caplan AI, *et al.* Mesenchymal cell- based repair of large, full-thickness defects of articular cartilage. J Bone Joint Surg Am 1994;76-A:579–92.
9. Butnariu-Ephrat M, Robinson D, Mendes DG, Halperin N, Nevo Z. Resurfacing of goat articular cartilage by chondrocytes derived from bone marrow. Clin Orthop 1998;330:234–43.
10. Steadman JR, Rodkey WG, Rodrigo JJ. Microfracture: surgical technique and rehabilitation to treat chondral defects. Clin Orthop 2001;391S:362–9.
11. Kumai T, Takakura Y, Higashiyama I, Tamai S. Arthroscopic drilling for the treatment of osteochondral lesions of the tarus. J Bone Joint Surg Am 1999;81-A: 1229–35.
12. Shea CM, Edgar CM, Einhorn TA, Gerstenfeld LC. BMP treatment of C3H10T1/2 mesenchymal stem cells induces both chondrogenesis and osteogenesis. J Cell Biochem 2003;90:1112–27.
13. Carlberg AL, Pucci B, Rallapalli R, Tuan RS, Hall DJ. Efficient chondrogenic differentiation of mesenchymal cells in micromass culture by retroviral gene transfer of BMP-2. Differentiation 2001;67:128–38.
14. Zuscik MJ, Baden JF, Wu Q, Sheu TJ, Schwarz EM, Drissi H, *et al.* 5-azacytidine alters TGF-beta and BMP signaling and induces maturation in articular chondrocytes. J Cell Biochem 2004;92:316–31.
15. Mason JM, Breitbart AS, Barcia M, Porti D, Pergolizzi RG, Grande DA. Cartilage and bone regeneration using gene-enhanced tissue engineering. Clin Orthop 2000; 379S:S171–8.
16. Issack PS, DiCesare PE. Recent advances toward the clinical application of bone morphogenetic proteins in bone and cartilage repair. Am J Orthop 2003;32: 429–36.
17. King GN. The importance of drug delivery to optimize the effect of bone morphogenetic proteins during periodontal regeneration. Curr Pharm Biotechnol 2001;2:131–42.
18. Fiedler J, Roderer G, Gunther KP, Brenner RE. BMP-2, BMP-4, and PDGF-bb stimulate chemotactic migration of primary human mesenchymal progenitor cells. J Cell Biochem 2002;87:305–12.
19. Postlethwaite AE, Raghow R, Stricklin G, Ballou L, Sampath TK. Osteogenic protein-1, a bone morphogenic protein member of the TGF-beta superfamily, shares chemotactic but not fibrogenic properties with TGF-beta. J Cell Physiol 1994;161:562–70.
20. Muckle DS, Minns RJ. Biological response to woven carbon fibre pads in the knee: a clinical and experimental study. J Bone Joint Surg Br 1989;71:60–2.
21. Buma P, Pieper JS, van Tienen T, van Susante JL, van der Kraan PM, Veerkamp JH, *et al.* Cross-linked type I and type II collagenous matrices for the repair of full-thickness articular cartilage defects-a study in rabbits. Biomaterials 2003;24:3255–63.
22. Cohen SB, Meirisch CM, Wilson HA, Diduch DR. The use of absorbable co-polymer pads with alginate and cells for articular cartilage repair in rabbits. Biomaterials 2003;24:2653–60.
23. Ushida T, Furukawa K, Toita K, Tateishi T. Three-dimensional seeding of chondrocytes encapsulated in collagen gel into PLLA scaffolds. Cell Transplant 2002;11:489–94.
24. Chiroff RT, White RA, White EW, Weber JN, Roy D. The restoration of the articular surfaces overlying Replamineform porous biomaterials. J Biomed Mater Res 1977;11:165–78.
25. Suominen E, Aho AJ, Vedel E, Kangasniemi I, Uusipaikka E, Yli-Urpo A. Subchondral bone and cartilage repair with bioactive glasses, hydroxyapatite, and hydroxyapatite-glass composite. J Biomed Mater Res 1996;32:543–51.
26. Miyamoto S, Takaoka K, Okada T, Yoshikawa H, Hashimoto J, Suzuki S, *et al.* Evaluation of polylactic acid homopolymers as carriers for bone morphogenetic protein. Clin Orthop 1992;278:274–85.
27. Saito N, Okada T, Horiuchi H, Murakami N, Takahashi J, Nawata M, *et al.* Biodegradable poly-D,L-lactic acid–polyethylene glycol blocks copolymers as a BMP delivery system for inducing bone. J Bone Joint Surg Am 2001;81-A:92–8.
28. Saito N, Okada T, Horiuchi H, Murakami N, Takahashi J, Nawata M, *et al.* A biodegradable polymer as a cytokine delivery system for including bone formation. Nat Biotechnol 2001;19:332–5.
29. Saito N, Okada T, Toba S, Miyamoto S, Takaoka K. New synthetic absorbable polymers as BMP carriers: plastic properties of poly-D,L-lactic acid–polyethylene glycol block copolymers. J Biomed Mater Res 1999; 47:104–10.
30. Tamai N, Myoui A, Tomita T, Nakase T, Tanaka J, Ochi T, *et al.* Novel hydroxyapatite ceramics with an interconnective porous structure exhibit superior osteoinduction *in vivo*. J Biomed Mater Res 2002; 59:110–7.
31. Nishikawa M, Myoui A, Ohgushi H, Ikeuchi M, Tamai N, Yoshikawa H. Bone tissue engineering using novel

interconnected porous hydroxyapatite ceramics combined with marrow mesenchymal cells: quantitative and three-dimensional image analysis. Cell Transplant 2004;13:367–76.
32. Kaito T, Myoui A, Takaoka K, Saito N, Nishikawa M, Tamai N, *et al.* Potentiation of the activity of bone morphogenetic protein-2 in bone regeneration by a PLA–PEG/hydroxyapatite composite. Biomaterials 2005;26:73–9.
33. Akita S, Tamai N, Myoui A, Nishikawa M, Kaito T, Takaoka K, *et al.* Capillary vessel network integration by inserting a vascular pedicle enhances bone formation in tissue-engineered bone using interconnected porous hydroxyapatite ceramics. Tissue Eng 2004;10:789–95.
34. Wei X, Gao J, Messner K. Maturation-dependent repair of untreated osteochondral defects in the rabbit knee joint. J Biomed Mater Res 1997;34:63–72.
35. Kumagai K, Saito T, Koshino T. Articular cartilage repair of rabbit chondral defect: promoted by creation of periarticular bony defect. J Orthop Sci 2003;8: 700–6.
36. Schaefer D, Martin I, Jundt G, Seidel J, Heberer M, Grodzinsky A, *et al.* Tissue-engineered composites for the repair of large osteochondral defects. Arthritis Rheum 2002;46:2524–34.
37. Ikeuchi M, Dohi Y, Horiuchi K, Ohgushi H, Noshi T, Yoshikawa T, *et al.* Recombinant human bone morphogenetic protein-2 promotes osteogenesis within atelopeptide type I collagen solution by combination with rat cultured marrow cells. J Biomed Mater Res 2002;60:61–9.
38. Hegyi L, Gannon FH, Glaser DL, Shore EM, Kaplan FS, Shanahan CM. Stromal cells of fibrodysplasia ossificans progressiva lesions express smooth muscle lineage markers and the osteogenic transcription factor Runx2/Cbfa-1: clues to a vascular origin of heterotopic ossification? J Pathol 2003;201:141–8.
39. Wakitani S, Imoto K, Yamamoto T, Saito M, Murata N, Yoneda M. Human autologous culture expanded bone marrow mesenchymal cell transplantation for repair of cartilage defects in osteoarthritic knees. Osteoarthritis Cartilage 2002;10:199–206.
40. Cook SD, Patron LP, Salkeld SL, Rueger DC. Repair of articular cartilage defects with osteogenic protein-1 (BMP-7) in dogs. J Bone Joint Surg Am 2003;85-A: 116–23.
41. Sellers RS, Peluso D, Morris EA. The effect of recombinant human bone morphogenetic protein-2 (rhBMP-2) on the healing of full-thickness defects of articular cartilage. J Bone Joint Surg Am 1997;79: 1452–63.
42. Hidaka C, Goodrich LR, Chen CT, Warren RF, Crystal RG, Nixon AJ. Acceleration of cartilage repair by genetically modified chondrocytes over expressing bone morphogenetic protein-7. J Orthop Res 2003;21: 573–83.
43. Sellers RS, Zhang R, Glasson SS, Kim HD, Peluso D, D'Augusta DA, *et al.* Repair of articular cartilage defects one year after treatment with recombinant human bone morphogenetic protein-2 (rhBMP-2). J Bone Joint Surg Am 2000;82:151–61.
44. Hunziker EB, Driesang IM, Morris EA. Chondrogenesis in cartilage repair is induced by members of the transforming growth factor-beta superfamily. Clin Orthop 2001;391S:171–81.
45. Frenkel SR, Saadeh PB, Mehrara BJ, Chin GS, Steinbrech DS, Brent B, *et al.* Transforming growth factor beta superfamily members: role in cartilage modeling. Plast Reconstr Surg 2000;105:980–90.
46. Kim HD, Valentini RF. Retention and activity of BMP-2 in hyaluronic acid-based scaffolds *in vitro*. J Biomed Mater Res 2002;59:573–84.
47. Inada M, Yasui T, Nomura S, Miyake S, Deguchi K, Himeno M, *et al.* Maturational disturbance of chondrocytes in Cbfa1-deficient mice. Dev Dyn 1999;214: 279–90.
48. Otto F, Thornell AP, Crompton T, Denzel A, Gilmour KC, Rosewell IR, *et al.* Cbfa1, a candidate gene for cleidocranial dysplasia syndrome, is essential for osteoblastic differentiation and bone development. Cell 1997;89:765–71.
49. de Crombrugghe B, Lefebvre V, Nakashima K. Regulatory mechanisms in the pathways of cartilage and bone formation. Curr Opin Cell Biol 2001;13:721–7.
50. Stricker S, Fundele R, Vortkamp A, Mundlos S. Role of Runx genes in chondrocyte differentiation. Dev Biol 2002;245:95–108.
51. Kim IS, Otto F, Zabel B, Mundlos S. Regulation of chondrocyte differentiation by Cbfa1. Mech Dev 1999; 80:159–70.
52. Lodie TA, Blickarz CE, Devarakonda TJ, He C, Dash AB, Clarke J, *et al.* Systematic analysis of reportedly distinct populations of multipotent bone marrow-derived stem cells reveals a lack of distinction. Tissue Eng 2002;8: 739–51.
53. De Ugarte DA, Alfonso Z, Zuk PA, Elbarbary A, Zhu M, Ashjian P, *et al.* Differential expression of stem cell mobilization-associated molecules on multi-lineage cells from adipose tissue and bone marrow. Immunol Lett 2003;89:267–70.
54. Shapiro F, Koide S, Glimcher MJ. Cell origin and differentiation in the repair of full-thickness defects of articular cartilage. J Bone Joint Surg Am 1993;75: 532–53.
55. Langer R. Drug delivery and targeting. Nature 1998; 392:5–10.
56. Jeong B, Bae YH, Lee DS, Kim SW. Biodegradable block copolymers as injectable drug-delivery systems. Nature 1997;388:860–2.

Available online at www.sciencedirect.com

SCIENCE DIRECT®

Advanced Drug Delivery Reviews 57 (2005) 1037–1048

Advanced DRUG DELIVERY Reviews

www.elsevier.com/locate/addr

Synthetic biodegradable polymers as drug delivery systems for bone morphogenetic proteins

N. Saito[a,*], N. Murakami[b], J. Takahashi[b], H. Horiuchi[b], H. Ota[b], H. Kato[b], T. Okada[c], K. Nozaki[d], K. Takaoka[e]

[a]*Department of Physical Therapy, Shinshu University School of Health Sciences, 3-1-1 Asahi, Matsumoto, Nagano 390-8621, Japan*
[b]*Department of Orthopaedic Surgery, Shinshu University School of Medicine, 3-1-1 Asahi, Matsumoto, Nagano 390-8621, Japan*
[c]*Research Institute, Taki Chemical Co., Ltd., 64-1 Nishiwaki, Befucho, Kakogawa, Hyogo 675-0125, Japan*
[d]*Applied Pharmacology Laboratories, Institute for Drug Discovery Research, Yamanouchi Pharmaceutical Co., Ltd., 21 Miyukigaoka, Tsukuba, Ibaraki 305-8585, Japan*
[e]*Department of Orthopaedic Surgery, Osaka City University Graduate School of Medicine, 1-5-7 Asahimachi, Abeno-ku, Osaka 545-0051, Japan*

Received 8 April 2004; accepted 30 December 2004

Abstract

Bone morphogenetic proteins (BMP) induce bone formation in vivo, and clinical application in repair of bone fractures and defects is expected. However, appropriate systems to deliver BMP for clinical use need to be developed. We synthesized a new synthetic biodegradable polymer, poly-D,L-lactic acid-para-dioxanone-polyethylene glycol block copolymer (PLA-DX-PEG), to serve as a biocompatible, biodegradable polymer for recombinant human (rh) BMP-2 delivery systems. In animal experiments, new bone was efficiently formed and a large bone defect was repaired using PLA-DX-PEG/rhBMP-2 composites. In addition, this new polymer could be used as an injectable delivery system for rhBMP-2. The rhBMP-2/PLA-DX-PEG composites also could be combined with other materials such as hydroxyapatite or titanium. This new synthetic polymer might be used for rhBMP-2 delivery in various clinical situations involving repair of bone, leading to great changes in orthopedic treatment.

Keywords: Bone formation; Bone repair; Fracture; Bone defect; Recombinant human bone morphogenetic protein-2; Tissue engineering

* Corresponding author. Tel./fax: +81 263 37 2409.
E-mail address: saitoko@hsp.md.shinshu-u.ac.jp (N. Saito).

0169-409X/$ - see front matter © 2005 Elsevier B.V. All rights reserved.
doi:10.1016/j.addr.2004.12.016

Contents

1. Introduction

The regeneration potential of human bone appears to be limited, given that repair of large bone defects such as those associated with comminuted fractures or bone tumor resection usually remains unrepaired [1]. Such cases have been treated routinely with autogeneic or allogeneic bone grafting. Major problems associated with autogeneic grafting include limited anatomic sources of donor bone and risk of morbidity from the additional surgery for procurement of the graft. In allogeneic bone grafting, major concerns are potential risks of transmission of disease, immunologic reaction of the host, poor osteogenic capacity of the transplanted bone, and high costs associated with a bone banking system [2–4]. Current examination of alternatives to grafting techniques suggests three possible new approaches to inducing new bone formation: implantation of certain cytokines such as bone morphogenetic proteins (BMP) in combination with appropriate delivery systems at the target site [5–7]; transduction of genes encoding cytokines with osteogenic capacity into cells at repair sites [8,9]; and transplantation of cultured osteogenic cells derived from host bone marrow [10–13]. In our estimation, the second approach represents the next major advance, while the third requires considerable additional resources and time to procure and culture cells. The first strategy appears to show the most practical promise for the near future. Appropriate delivery systems are essential to this technique. In this review, we outline the development of new delivery systems for BMP and preclinical animal experiments concerning bone tissue regeneration that suggest clinical applications.

2. Bone morphogenetic proteins (BMP) and delivery systems

2.1. BMP

BMP induce new bone formation by directing mesenchymal stem cells toward chondroblastic and osteoblastic differentiation, and causing them to proliferate in vivo. BMP expression has been confirmed to occur at the initial stage of the fracture healing process, and to participate in a cascade regulating bone repair processes. Also, new bone can be induced to form heterotopically, such as when the BMP are implanted in muscle in animal models using appropriate delivery systems. These observations suggest that BMP could be applied clinically to promotion of repair of bone.

BMP were first characterized in 1965 by Urist as a biologically active molecule inducing new ectopic bone formation from decalcified bone matrix in vivo [14]. A cDNA encoding BMP was cloned by Wozney